國立臺灣大學工學院化學工程研究所

碩士論文

Graduate Institute of Chemical Engineering
College of Engineering
National Taiwan University

Master Thesis

具有酸鹼官能基之中孔洞氧化矽奈米催化劑之合成及其於纖維素轉換至羥甲基糠醛之應用

Acid-Alkaline Bi-functionalized Mesoporous Silica Nanocatalysts for Direct Cellulose-to-HMF Conversion

彭文暉

Wun-Huei Peng

指導教授：吳嘉文 博士

Advisor: Kevin Chia-Wen Wu, Ph.D.

中華民國 100 年 7 月

July, 2011

國立臺灣大學碩士學位論文
口試委員會審定書

具有酸鹼官能基之中孔洞氧化矽奈米催化劑之合成及其於纖維素轉換至羥甲基糠醛之應用

Acid-Alkaline Bi-functionalized Mesoporous Silica Nanocatalysts for Direct Cellulose-to-HMF Conversion

本論文係 彭文暉君（學號 R98524077）在國立臺灣大學化學工程研究所完成之碩士學位論文，於民國一〇〇年七月八日承下列考試委員審查通過及口試及格，特此證明

口試委員：

_____（指導教授）

_____

_____

_____

_____

_____

系主任、所長 _____（簽名）

誌謝

首先在我的碩士研究生涯中，我要感謝吳嘉文教授亦師亦友的指導與栽培，讓我學習到如何做好口頭報告、寫作技巧以及對實驗負責任的態度。有老師的砥礪和幫助，本論文才能順利完成。同時，也要感謝國科會計畫提供實驗經費，使研究能夠順利進行。

兩年左右的碩士班生活，感謝偉航在生質能以及 HPLC 使用的教導；感謝盈瑩在實驗和文書處理的幫忙；感謝永和常與我討論實驗；感謝義榮、丫花與我分享一些生活趣事；感謝一起畢業的同學智澎、雅惠的互相幫助；感謝實驗室的全體同仁，讓實驗室隨時充滿歡樂的氣氛。

最後，感謝親愛的女友願意包容我的固執，耐心地分擔我所有的情緒；感謝親愛的家人，無怨無悔的支持與鼓勵。

國立台灣大學工學院化學工程學所

中孔徑奈米材料實驗室

彭文暉

摘要

本研究探討了具有大孔洞與不同酸、鹼官能基之中孔洞奈米催化劑 (LPMSN, LPMSN-NH_2, LPMSN-SO_3H and LPMSN-Both) 之合成及其於纖維素一步轉換至羥甲基糠醛 (5-Hydroxymethylfurfural, 5-HMF) 之應用。羥甲基糠醛是非常有價值的化合物可應用於合成高分子和燃料添加物。由於能源危機的議題，發展新的替代再生能源(如生質能)已變成一個很重要的課題。將木質纖維素轉換至羥甲基糠醛，主要牽涉了三個反應步驟。(1)利用酸催化劑使多醣類降解至葡萄糖；(2)利用鹼催化劑使葡萄糖進行異構化反應轉換至果糖；(3)利用酸催化劑使果糖進行脫水反應轉換至羥甲基糠醛。果糖轉換至羥甲基糠醛的結果顯示，酸催化劑 (LPMSN-SO_3H) 可以有效促使果糖的脫水反應，進而產出 70.53%的羥甲基糠醛。葡萄糖轉換至羥甲基糠醛的結果顯示，具有胺官能基的鹼、酸鹼催化劑 (LPMSN-NH_2 and LPMSN-Both) 可以有效促使葡萄糖的異構化反應，進而生成了 13.27 和 13.77%的羥甲基糠醛。纖維雙糖轉換至羥甲基糠醛的結果顯示，酸催化劑 (LPMSN-SO_3H) 可以有效促使纖維雙糖的水解反應，進而產生 18.93%的羥甲基糠醛。纖維素轉換至羥甲基糠醛的結果顯示，酸、酸鹼催化劑 (LPMSN-SO_3H and LPMSN-Both) 整體上皆約有 57%的總產率，其中酸催化劑 (LPMSN-SO_3H) 又可催化纖維素產生 19.23%的羥甲基糠醛。我們確信合成出中孔洞氧化矽奈米催化劑可以有效的應用在纖維素一步轉換至羥甲基糠醛。

關鍵字:中孔洞奈米材料、酸鹼催化劑、離子液體、纖維素、羥甲基糠醛。

Abstract

This study reports a one-pot strategy to produce 5-hydroxymethylfurfural (5-HMF, a very useful chemical for many polymers and fuel additives) with the presence of acid (SO_3H), alkaline (NH_2) and acid-alkaline (SO_3H and NH_2) bi-functionalized mesoporous silica nanoparticles with large pores (namely, LPMSN-SO_3H, LPMSN-NH_2 and LPMSN-NH_2-SO_3H, respectively) as heterogeneous solid catalysts. Due to the crisis of energy, developing an alternative energy such as biomass energy has become an important issue. To convert lignocellulosic biomass (e.g. cellulose, cellobiose and glucose etc.) into 5-HMF, there are three major steps: (1) depolymerization of polysaccharide (cellulose) into glucose with the presence of an acid catalyst; (2) isomerization of glucose into fructose with the presence of an alkaline catalyst; (3) dehydration of fructose into 5-HMF with the presence of an acid catalyst. The results for fructose-to-HMF conversion showed that the LPMSN-SO_3H catalysts could promote the dehydration of fructose to 5-HMF with a high yield of 70.53%. For glucose-to-HMF conversion, the result indicated that both the LPMSN-NH_2 and LPMSN-NH_2-SO_3H catalysts could efficiently enhance isomerization of glucose to 5-HMF with a high yield of 13.27 and 13.77%, respectively. For cellobiose-to-HMF conversion, the results pointed out that the LPMSN-SO_3H catalysts could promote the hydrolysis of cellobiose and yield the maximum amount of 5-HMF (i.e., approximately 18.93%). For the cellulose-to-HMF conversion, the results indicated that both of the LPMSN-SO_3H and LPMSN-NH_2-SO_3H catalysts exhibit the highest yield of overall products (cellobiose, glucose and 5-HMF) approximately 57%, where the LPMSN-SO_3H catalysts could produce the highest yield of 5-HMF (i.e., 19.23%). We believe that the synthesized mesoporous solid catalysts are useful for one-pot production of 5-HMF from cellulose.

Keywords: mesoporous silica nanoparticles, acid-alkaline catalyst, ionic liquids, cellulose, 5-hydroxymethylfurfural.

Table of Content

List of Figure

List of Table

Chapter 1 Introduction

1.1 Introduction of mesoporous silica nanoparticles

Nanoscience and nanotechnology are extensively studied and developed in recent years. Scientists have developed lots of technologies and have used them for the fabrication of novel materials, the surface modifications. In general, these technologies are divided into two parts, top-down and bottom-up approaches. According to the classification made by IUPAC [1], porous materials could be classified in three categories, depending on their pore size (diameter, d), in micro- ($d < 2$ nm), meso- (2 nm $< d < 50$ nm), and macroporous materials ($d > 50$ nm). The pore size of the materials in this study is in the range of 2-50 nm, so they are classified as mesoporous materials.

Table 1.1 Definition of porous materials

Name	Pore diameter
Microporous	$d < 2$ nm
Mesoporous	2 nm $< d < 50$ nm
Macroporous	$d > 50$ nm

As early as 1950s, porous materials are originally studied for catalysis and adsorption applications, due to their high surface area, hydrothermal stability and catalytic properties. One of the typical material is zeolite, they are extensively used as selective ion-exchange agents and adsorbents in industrial catalytic processes [2]. In 1990s, there are two groups reported a new discovery of silica materials with a larger pore size materials. One is the Kresge group working at Mobil Oil Corporation, USA [3], and the other is the Kuroda group at Waseda University, Japan [4]. Kresge et al. reported the

mesoporous silica nanoparticles could be synthesized by introducing supramolecular assemblies as templating agents, and the inorganic species in solution could cooperatively assemble with those micelles. They also produce a series of mesoporous materials called M41S family, including MCM-41, MCM means Mobil composition of Matter, (hexagonal phase), MCM-48 (cubic phase) and MCM-50 (lamellar phase).

Generally, micellar aggregates could organize into different shapes such as sphere, cylinder, planar bilayer and so on, as shown in **Figure 1.1a** [5].

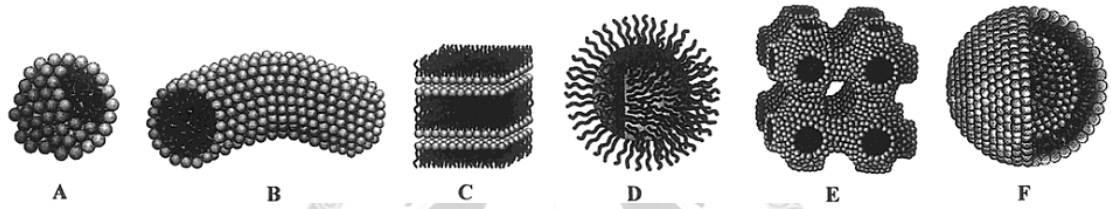

Figure 1.1a Different shapes of micelle: A = sphere, B = cylinder, C = planar bilayer, D = reverse micelles, E = bicontiuous phase, F = liposomes.

Typically, the porous materials are composed of organic (surfactant) and inorganic component. Surfactant is composed of hydrophobic tail and hydrophilic head. Commonly, the hydrophobic tail is formed from a long carbon chain or hydrophobic polymer and the hydrophilic head is formed of polar, ionic atoms and polymer. According to the hydrophilic head, the surfactant could be classified into the two parts: (1) Ionic type such as cationic, anionic and zwitterionic surfactant; (2) nonionic type such as Fatty alcohols, Polyoxyethylene glycol alkyl ethers and Polyoxypropylene glycol alkyl ethers.

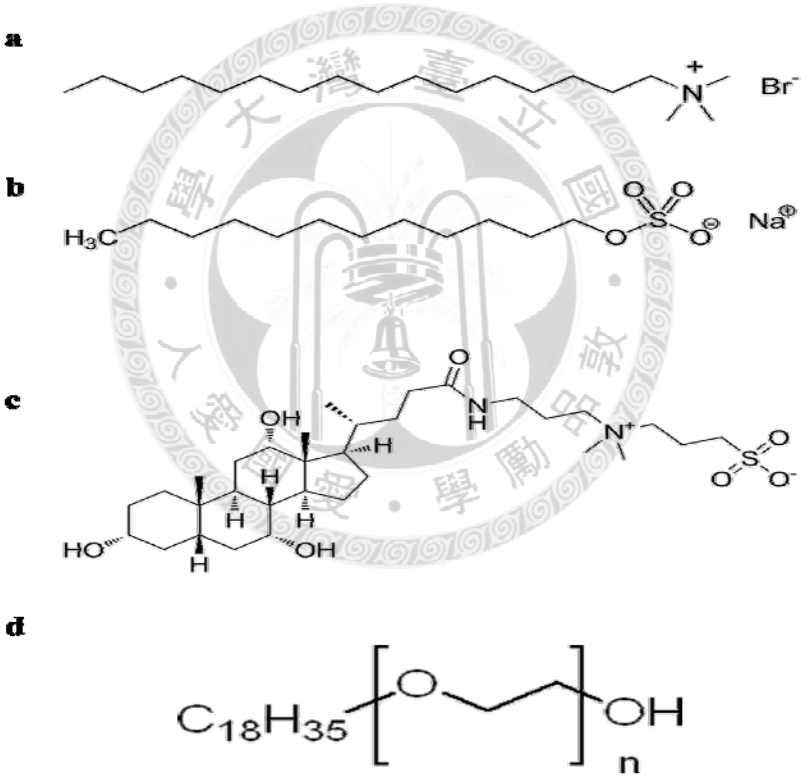

Figure 1.1b Different types of surfactant:

a cationic surfactant (cetyl trimethylammonium bromide),

b anionic surfactant (sodium lauryl sulfate), c zwitterionic surfactant

(3-[(3-cholamidopropyl)dimethylammonio]-1-propanesulfonate,

d nonionic surfactant (Brij 97)

The formation of mesoporous materials are sorted into two principal approaches.

(1) Liquid-crystal mechanism (LCT) [3]

(2) Cooperative self-assembly mechanism (CSA) [6]

Both mechanisms are shown in **Figure 1.1c**.

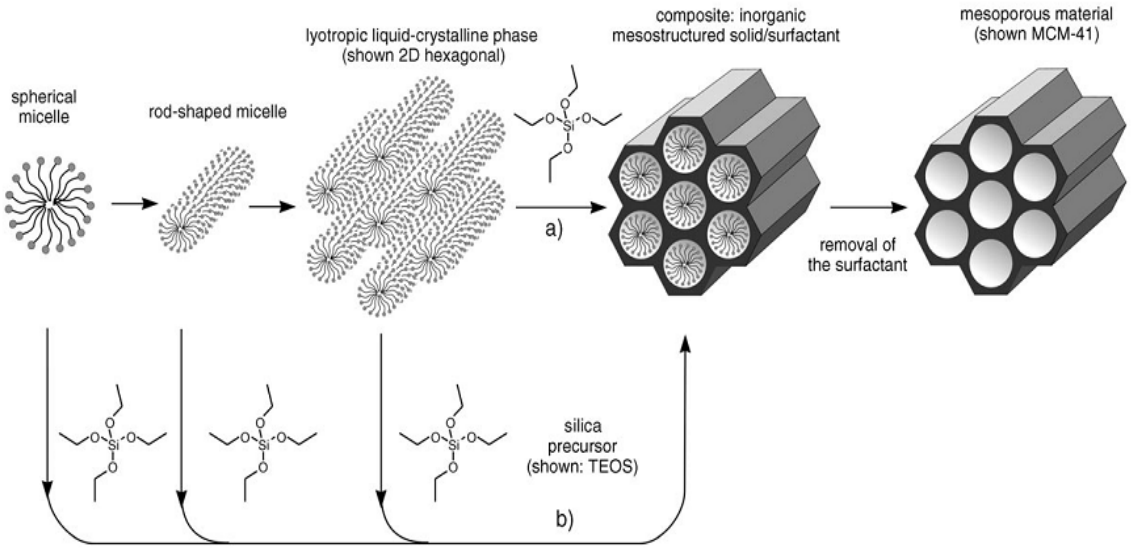

Figure 1.1c Two pathways of formation of mesoporous materials [7]: a) liquid-crystal mechanism (LCT), b) cooperative self-assembly mechanism (CSA)

The interaction between the organic (surfactant) and inorganic (silica source) is shown in figure 1.1d [8].

For the upper four the interaction between the organic and inorganic species is electrostatic nature. For bottom two the interaction between organic and inorganic species is the hydrogen bonding.

S^+I^-: Under the basic condition, silica sources as the anions and quaternary ammonium surfactants as the cations.

S^-I^+: Under acidic condition, silica source (positive charge) as the cations and the surfactant as the anions.

$S^+X^-I^+$: Under the acidic condition, silica sources (positive charge) require a mediator ion (usually are halide) to ensure the interaction between cationic surfactant.

$S^-M^+I^-$: Under basic condition, silica sources (negative charge) require a mediator ion ($M=Na^+$, K^+) to ensure the interaction between anionic surfactant.

S^0I^0: Under the pH~2 condition, silica sources (no charge) and the interaction between both of them are hydrogen bonding.

$S^0(IX)^0$: Under the acidic condition, the silica sources (positive charge) need adding some anionic ions to make it neutral. Then, the complex interacts with surfactant by hydrogen bonding.

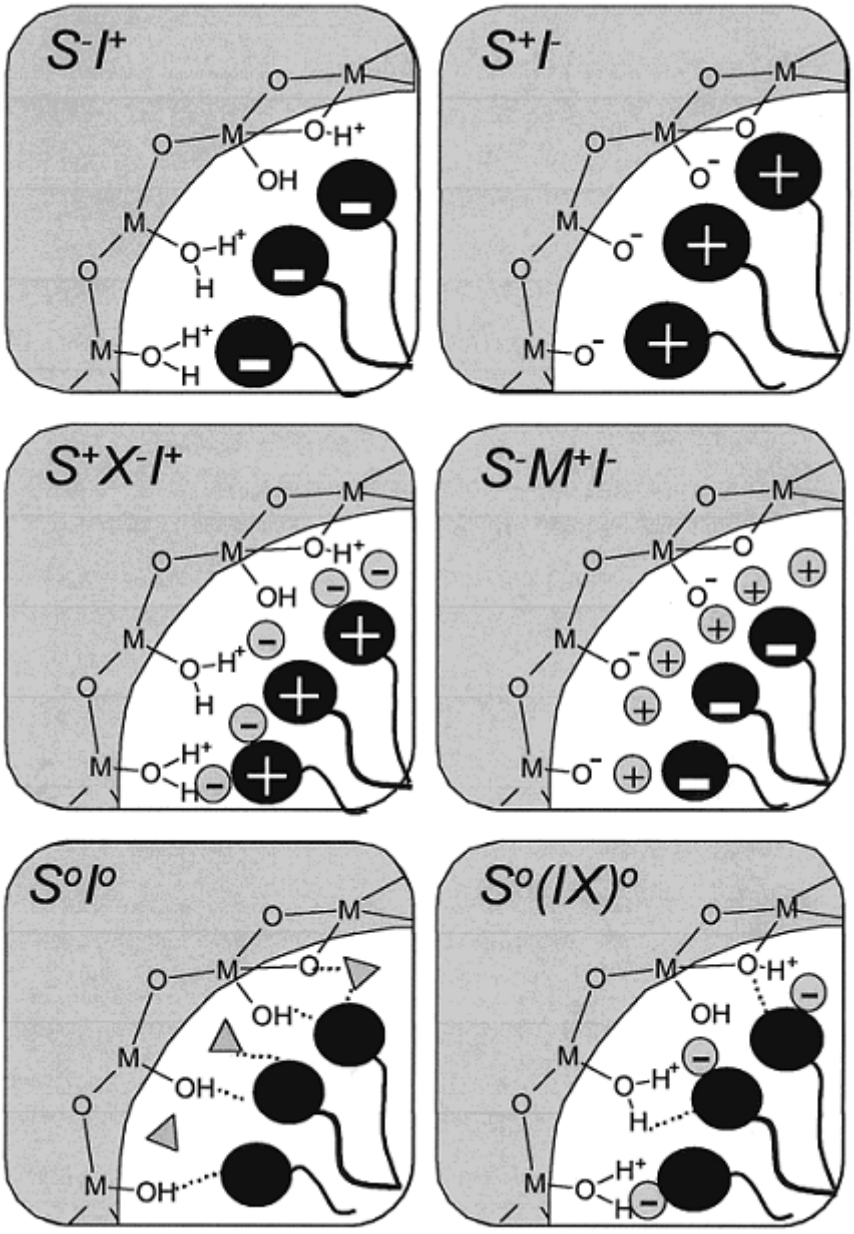

Figure 1.1d Different interaction between silica and surfactant interfaces. S: surfactant, I inorganic species. M^+ and X^-: counterions.

1.1-1 Ultra-large pore sizes mesoporous silica materials

In order to solve the problem that microporous materials couldn't satisfy the applications involving large molecules. Numerous researches have been made in developing ultra-large pore sizes mesoporous silica materials. Since 1990s, the two groups[3, 4] discovery the new mesoporous silica materials, a variety of mesoporous silica materials with larger pore size have been synthesized such as SBA-n [9], SBA-15 [10], FDU-12 [11], Si-FDU-18 [12] and MCF [13-15]. Conventional syntheses of large pore size mesoporous materials have the following two strategies: (1) Using surfactant with high molecular weights as templates [12]; (2) adding hydrophobic additives as swelling agents (e.g. TMB, 1,3,5-trimethylbenzene) [11, 13, 15, 16]. However, these two strategies still have the small shortages. For instance, using surfactants with high molecular weights as templates to synthesize mesoporous materials often have the cage structures with the entrance effects [11, 12]. The addition of TMB results in the formation of silica cellular foams with thin shells [13, 15].

In this study we modified a published paper to synthesize mesoporous silica materials with ultra-large pore size [17]. It used Brij-97 as templates and dimethyl o-phthalate as swelling agent in a neutral pH system to form spherical mesoporous silica nanoparticles with interconnected mesoscale channels with diameter 40 nm. The possible mechanism for the formation of mesoporous silica materials with ultra-large pores in a neutral pH system was shown in **Figure 1.1-1**.

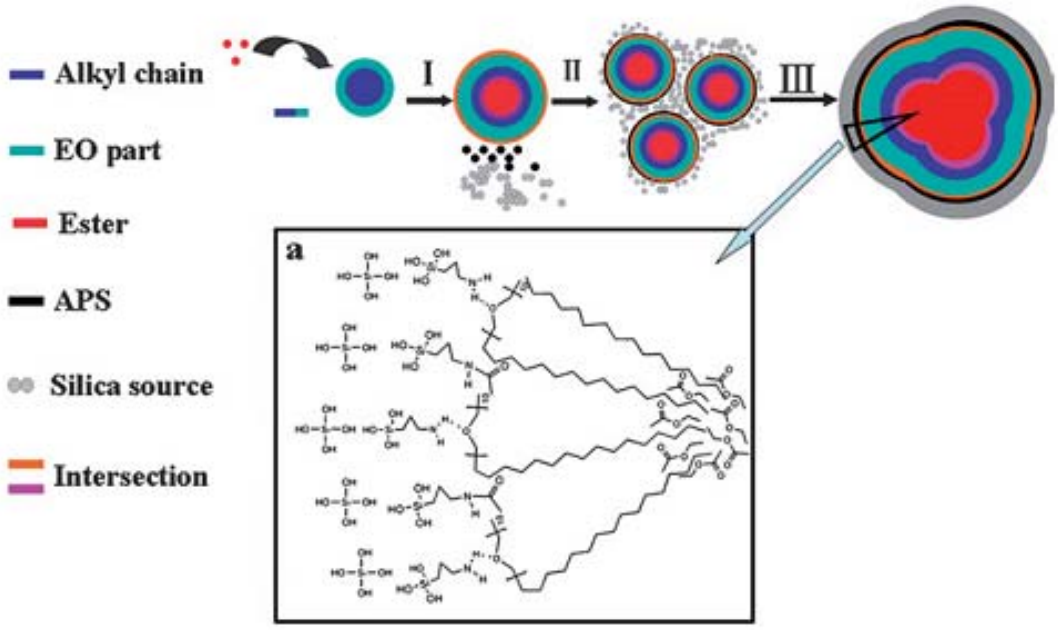

Figure 1.1-1 Possible mechanism for the formation of mesoporous silica materials with ultra-large pores in a neutral pH system

1.2 Introduction of biomass energy

1.2-1 Evolution of biofuels

The shortage of fossil fuels results in the serious following problems:

1. The storage of fossil fuels is getting smaller and smaller, but the usage of it is getting more and more. This will cause the energy crisis and bring many problems.
2. The greenhouse gases are accompanied with burning fossil fuels. The rate of emission is growing highly, it causes the global warming.
3. As the result of that, it's time to develop an innovative energy to replace the fossil fuels.

We could learn a lot of things from fossil fuels. An innovative energy must have the unique character renewable. There are many renewable energy such as solar, hydraulic, wind power and biomass energy. Biomass energy not only could achieve the sustainable development, but also solve the problem of fossil fuels derivatives.

The evolution of biomass energy is from 1st to 4th generation biofuels. The 1st generation biofuels are commonly made from sugar, starch and vegetable oil. Bioethanol is the most representative biofuels of this generation and are fermented from sugar and starch. The alcohol-from-corn is the most popular way of bioethanol production, but there is a fatal problem of this method. The transportation fuel will compete with food and finally it will get the food deficiency. The 2nd generation biofuels could solve the problem of the 1st generation biofuels and could supply a larger proportion of our fuel supply sustainably and with better environmental benefits. The raw materials of 2nd generation biofuels are from woods, biomass wastes and agricultural residues. The major component of the biomass is lignocelluloses which are composed of cellulose, hemicelluloses and lignin. The 3rd generation biofuels are

derived from algae (so-called algae fuel). Due to high capital and operating cost for cultivating algae, the 3rd generation biofuels still have a long way to go. The 4th generation biofuels is not clearly defined now, but some have referred to it as the biofuels created from processes other than 1st, 2nd and 3rd generation methods. Herein, this study focuses on synthesizing 5-hydroxymethylfurfural, a fine chemical platform, and is classified as 2nd generation biofuels.

1.3 Literature review of biomass energy

The major component of biomass (lignocelluloses) is mainly divided into three parts [18]:

(1) Cellulose: linear polysaccharides, consisting of D-glucose through β-1,4-glycosidic bonds.

(2) Hemicelluloses: A copolymer of any of monosaccharides glucose, galactose, mannose, xylose, arabinose and glucuronic acid).

(3) Lignin: a very complex 3-D polymer of different phenylpropane units bound together by ether and carbon-carbon bounds.

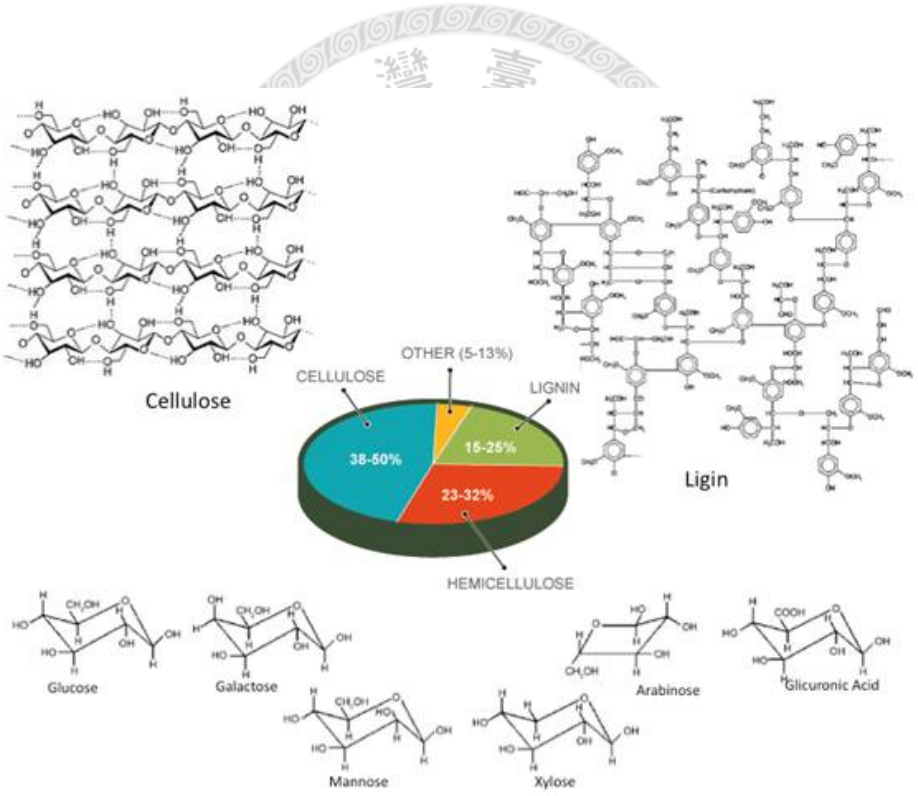

Figure 1.3 Composition of lignocelluloses: cellulose, hemicelluloses, and lignin.

1.3-1 Reaction pathways of synthesis of 5-HMF

5-HMF could be synthesized from hexose and there are two reaction pathways of hexose converted into 5-HMF [19]. As shown in **Figure 1.3-1**, one of the reaction pathways undergoes the open chain reaction via acyclic intermediates and the other reaction pathway undergoes the ring structure reaction via cyclic intermediates.

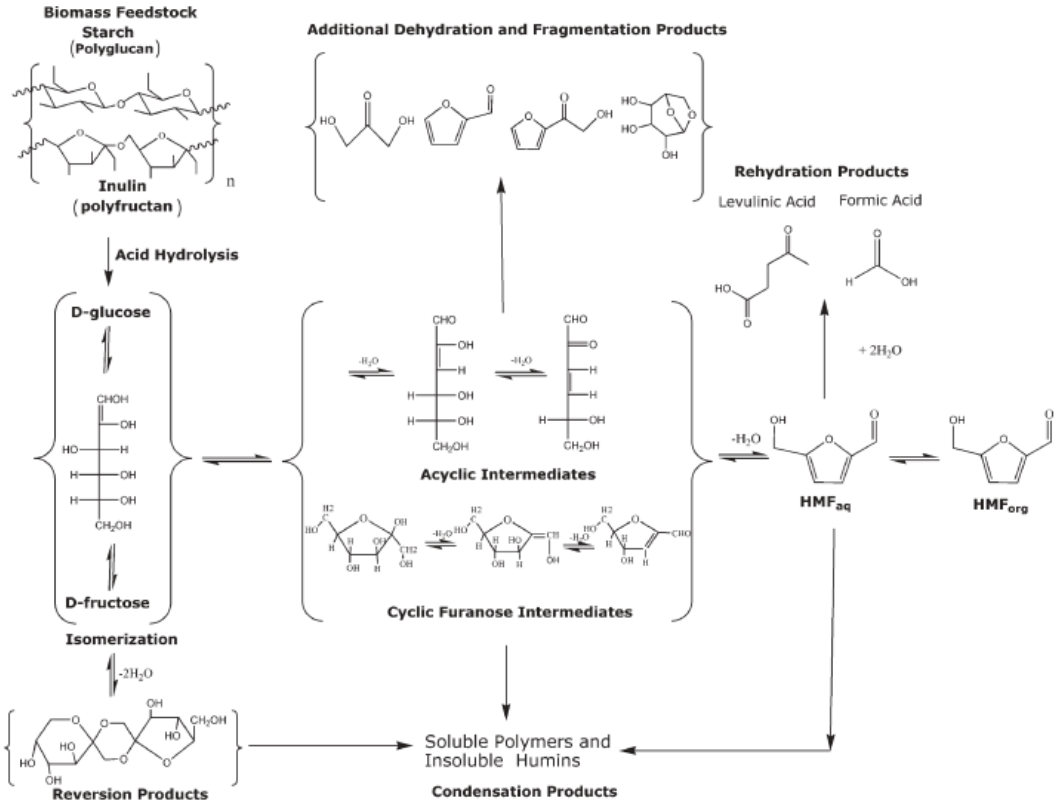

Figure 1.3-1 Reaction pathways of hexose converted into 5-HMF.

1.3-2 Application of 5-HMF

5-Hydroxymethylfurfural (5-HMF) is a fine chemicals with wide applications, it could be further manufactured to different derivatives (e.g. 2,5-DMF, 2,5-BHF, 2,5-FDCA and 2,5-DFF).

2,5-Dimethylfuran (2,5-DMF) [20] was formed from hydrogenation of 5-HMF. The representative application is transportation fuels. Comparison with ethanol the energy density is 31.5 MJ/L larger than ethanol (23MJ/L). By the way the energy density of gasoline is 35 MJ/L, 2,5-DMF has a great potential to substitute gasoline. Besides energy density, 2,5-DMF also has the other advantages such as insoluble in water and low volatility.

2,5-Bis(hydromethyl)furan (2,5-BHF) [21] was formed from hydrogenation of 5-HMF. The application of 2,5-BHF is to synthesize polymers.

2,5-Furandicarboxylic acid (2,5-FDCA) [22] was formed from oxidation of 5-HMF. The application of 2,5-FDCA is fungicide. 2,5-FDCA also could substitute terephthalic acid, a widely used component in synthesis of polyesters and be the starting materials for the production of succinic acid.

2,5-Diformylfuran (2,5-DFF) [23] was formed from oxidation of 5-HMF. The application of 2,5-DFF is synthesis of polymer and as intermediates of pharmaceuticals.

1.3-3 Synthesis of 5-HMF from different starting materials

According to the starting materials of synthesis of 5-hydroxymethylfurfural, we will introduce it from mono- to polysaccharides.

1.3-3a Fructose

5-Hydroxymethylfurfural (5-HMF) was first yielded from the mixture of fructose in the presence of oxalic acid [24]. From the first oxalic acid-catalyzed synthesis of 5-HMF, there are tremendously different kinds of acid have been found as catalyst for synthesis of 5-HMF. The following work, Antal et al. proved that 5-HMF was synthesized from fructose through removing three water molecules in the presence of acidic medium [25]. They also reported the dehydration of fructose with sulfuric acid as catalyst in the supercritical reactor at 250 ºC could yield approximately 53% of 5-HMF. Roman-Leshkov et al. provided a bi-phasic system with HCl or ion-exchange resin as catalyst [26]. As shown in **Figure 1.3-3a**, fructose was dehydrated into 5-HMF in the aqueous solution and the 5-HMF was continuously extracted into methylisobutylketone (MIBK) modified with 2-butanol to enhanced the partition ability. The same group also reported in the bi-phasic system with saturated salt could improve the ability of extraction [27].

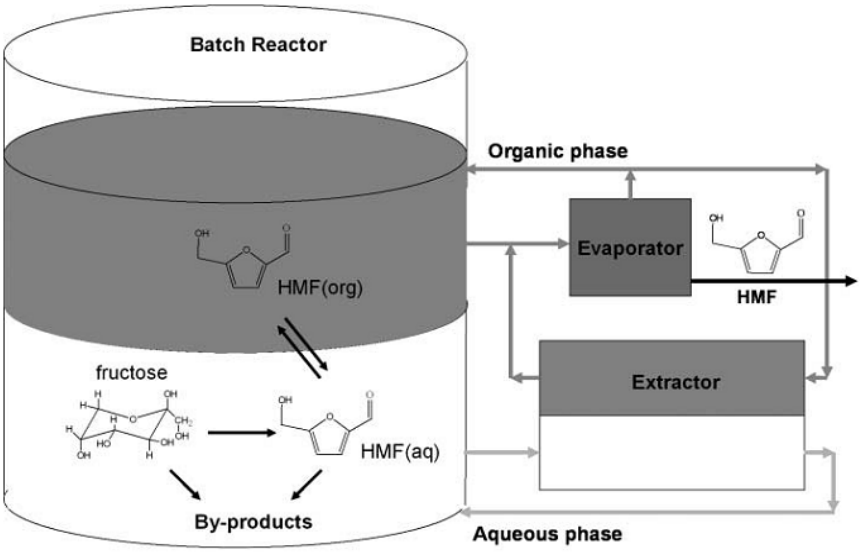

Figure 1.3-3a Synthesis of 5-HMF from fructose using biphasic system

Moreau et al. investigated the series of H-form mordenites as catalyst at 165 ºC in the mixture of water and methylisobutylketone and observed the Si/Al ratio of 11 is the most effective one to dehydrate fructose [28]. They also found the conversion of fructose and the selectivity of 5-HMF depend on the acidic and structural properties of the H-form mordenite. Ilgen et al. reported the Amberlyst-15 as catalyst at 100 ºC in the mixture of choline chloride and fructose could yield 40% 5-HMF [29]. Lansalot-Matras and Moreau tested the dehydration of fructose in the two different kind of ionic liquids with Amberlyst-15 as catalyst. The yield of 5-HMF in the 1-butyl-3-methylimidazolium tetrafluoroborate ([BMIM]BF_4) was 52% within 3 h and in the 1-butyl-3-methyl -imidazolium hexafluorophosphate ([BMIM]PF_6) was close to 80% within 24 h [30]. Qi et al. studied the dehydration of fructose into 5-HMF in the mixture of acetone and water with cation exchange resin (Dowex 50wx8-100) as catalyst [31]. The yield of 5-HMF was 73.4% for 94% conversion at 150 ºC. Moreau et al. studied the dehydration of fructose with the presence of 1-H-3-methylimidazolium chloride ([HMIM]Cl) acting both as solvent and catalyst at 90 ºC and yield 92% of 5-HMF within 15-45min[32].

1.3-3b Glucose

5-HMF also could be synthesized from glucose, the most abundant and inexpensive feedstock, but glucose has been reported to have lower reaction rate and lower selectivity to 5-HMF compared to fructose. This result is due to the stable ring structure of glucose. As the above mentioned the straightforward method to synthesize 5-HMF is from fructose. Isomerization of glucose to fructose is known as the Lobry-de Bruyn-van Ekenstein transformation and is generally catalyzed by base. Takagaki et al. reported a strategy of one-pot reaction for synthesizing 5-HMF. At the former stage (0 to 2.5h) the isomerization of glucose into fructose was at 100 ºC in the presence of N,N-dimethylformamide (DMF) with the Mg-Al hydrotalcite (HT) as catalyst [33, 34]. The later stage (2.5 to 4.5 h) the dehydration of fructose into 5-HMF was adding Amberlyst-15 as catalyst. This method could yield approximately 45% of 5-HMF from glucose. There is a similar strategy, Huang et al. proposed a combination of glucose isomerase and HCl was employed as the catalyst and the reaction was performed in the mixture of water and butanol biphasic reactor [35]. The yield of 5-HMF from this method is 63.3%. Chidambaram and Bell investigated a nearly 100% yield of 5-HMF could be reached with 12-molybdophosphoric acid (12-MPA) as catalyst in the mixture of 1-ethyl-3-methylimidazolium chloride ([EMIM]Cl) and acetonitrile [20]. They also have proposed a glucose dehydration process via ring opening of the pyranose form of glucose to explain this acid catalyzed, as shown in **Figure 1.3-3b**.

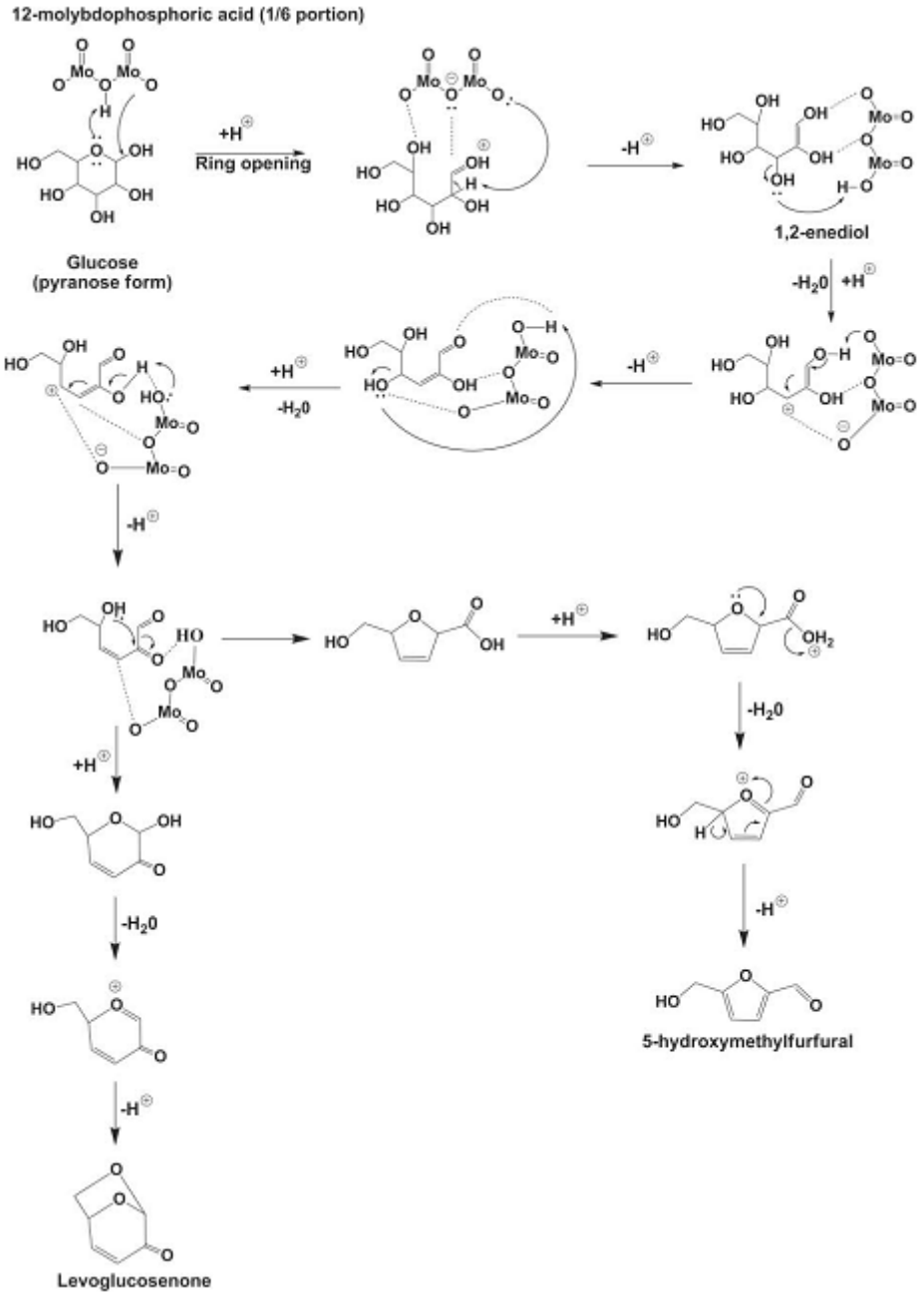

Figure 1.3-3b Proposed mechanism of glucose-to-HMF with the presence of acid catalyst

Zhao et al. found the metal halide ($CrCl_2$) played a important role in dehydrating glucose into 5-HMF in the presence of 1-ethyl-3-methylimidazolium chloride ([EMIM]Cl) at 100 ºC for 3 h [36]. They proposed a mechanism to explain it as shown in **Figure 1.3-3c**. The mixture of $CrCl_2$ and [EMIM]Cl will form a complex ($EMIMCrCl_3$), a important compound to induce the mutarotation and isomerization reaction of glucose to form 5-HMF.

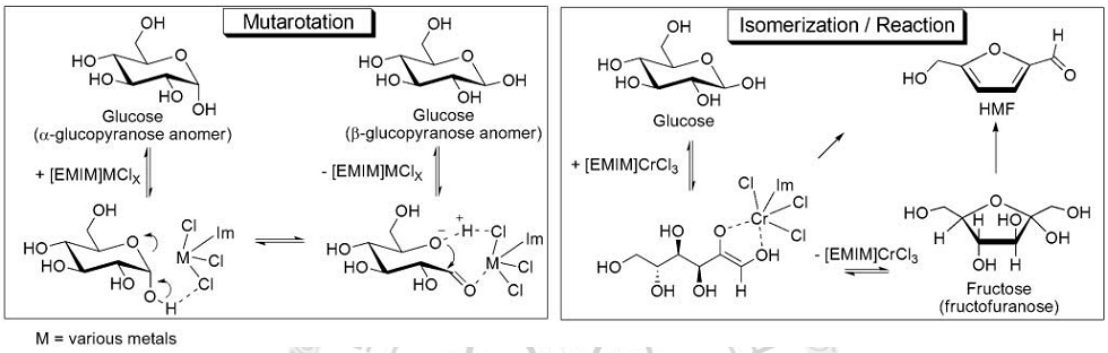

Figure 1.3-3c Mechanism of mutarotation and isomerization with the presence of $CrCl_2$ and [EMIM]Cl

Hu et al. investigated the dehydration of glucose in the presence of 1-ethyl-3-methylimidazolium tetrafluoroborate ([EMIM]BF_4) with the $SnCl_4$ as catalyst at 100 ºC for 3 h. The yield of 5-HMF could reach 61% [37]. They also indicated the Sn atom and glucose will form a chelate complex, an important complex in the synthesis of 5-HMF, and proposed a mechanism of this reaction.

1.3-3c Cellulose

Cellulose exists a lot of inter- and intra-molecular hydrogen bond and form a very crystalline structure. Due to the above reason, cellulose is difficultly dissolved in water and most of organic/inorganic solvent. Even though cellulose is very prospective, it is the major component of lignocelluloses and the uniform structure (β-(1,4) linked D-glucose units). So there are several pretreatments of cellulose, including physical, physic-chemical, chemical and biological processes [38]. Physical pretreatment include mechanical comminution and pyrolysis. Physic-chemical pretreatment include steam, CO2 and ammonia fiber explosion (AFEX). Chemical pretreatment include ozonolysis, acid and base hydrolysis. Biological pretreatment include microorganisms and enzymes hydrolysis. Earlier in 1934, there is innovative method with the presence of ionic liquid have attracted lots of attention on the dissolution of cellulose [39]. Graenacher discovered that molten N-ethylpyridinium chloride, in the presence of nitrogen-containing bases, could be used to dissolve cellulose. Ionic liquid is composed of an organic cation and anion (e.g. halide, BF_4^-, PF_6^- etc.). Ionic liquid has many benefits as a solvent in cellulosic conversion such as low melting point (room temperature ionic liquid, below 100 ºC), chemical and thermal stability and low volatility [40]. Recently Remsing et al. reported the 1-n-butyl-3-methylimidazolium chloride could disrupt the hydrogen bonding inside the cellulose [41]. This also provides a new strategy to dissolve cellulose without raising temperature and pressure. Su et al. have successfully been performed a single step conversion of cellulose with a pair of metal chlorides ($CrCl_2$ and $CuCl_2$) as catalyst in the 1-ethyl-3-methylimidazolium chloride at 120 ºC for 8 h [42]. The best yield of 5-HMF is approximately 54% while adding the paired $CuCl_2/CrCl_2$ catalyst at the mole ratio of $CuCl_2$ is equal to 0.17. Qi et al. reported an efficient method for converting cellulose

into 5-HMF in the presence of $CrCl_3$ as catalyst and 1-butyl-3methylimidazolium chloride as solvent at 150 ºC for 10 min [43]. The yield of 5-HMF is 54% and the mixture of ionic liquid and $CrCl_3$ could be reused with six cycles. Zhang and Zhao found the microwave-assisted conversion of cellulose into 5-HMF with the yield of 62% within 2.5 min. Binder and Raines reported that N,N-dimethylacetamide (DMA) containing lithium chloride (LiCl) is a privileged solvent that enables the synthesis of 5-HMF from cellulose [44]. For example the 54% 5-HMF yield from cellulose was obtained in the presence of DMA-LiCl with $CrCl_2$ and HCl as catalyst at 140 ºC for 2 h.

1.3-3d The other mono-, di- and polysaccharide

There are lots of di- and polysaccharide also could be the starting material of synthesis 5-HMF such as sucrose, cellobiose, starch and inulin. Chheda et al. reported the biphasic reactor could get a good selectivity of 5-HMF at high conversions from sucrose, cellobiose and starch [19]. The reaction system composed of the mixture of water and DMSO in the aqueous phase and the mixture of MIBK and 2-butanol in the organic phase with HCl as catalyst at 170 ºC. Takagaki et al. also reported that a pair of solid acid and base could use in the formation of furfural from xylose [45]. The similar strategy of the formation of 5-HMF from glucose combine a isomerization and a dehydration step.

Chapter 2 Motivation

In this study we try to synthesize a kind of catalyst material containing two different functionalities and use it to do the lignocellulosic conversion. To convert lignocellulosic biomass (e.g. cellulose, cellobiose and glucose etc.) into 5-HMF, there are three major steps: (1) depolymerization of polysaccharide (cellulose) into glucose with the presence of an acid catalyst; (2) isomerization of glucose into fructose with the presence of an alkaline catalyst; (3) dehydration of fructose into 5-HMF with the presence of an acid catalyst. We aim to synthesize ultra large pore size mesoporous silica nanocatalysts (LPMSN) with different kinds of functionalities (LPMSN-NH_2 and LPMSN-SO_3H and H_3OS-LPMSN-NH_2). We aim to use these catalysts to yield the highest 5-HMF.

Chapter 3 Materials and experimental methods

3.1 Chemicals

Name	Formula	Supplier
Brij ® 97	$C_{38}H_{76}O_{11}$	Sigma
(3-Aminopropyl)trimethoxysilane, 97%	$H_2N(CH_2)_3Si(OCH_3)_3$	Aldrich
Dimethyl phthalate 99+%	$C_{10}H_{10}O_4$	Aldrich
Tetraethyl orthosilicate, Reagent Grade, 98%	$Si(OC_2H_5)_4$	Aldrich
Toluene, 99.8%, extra dry, over Molecular Sieves, AcroSeal ®	$C_6H_5CH_3$	Acros
Toluene	$C_6H_5CH_3$	Mallinckrodt Chemicals
(3-Mercaptopropyl)trimethoxysilane, 95%	$HS(CH_2)_3Si(OCH_3)_3$	Alfa Aesar
3-Mercaptopropionic acid	$HS(CH_2)_2COOH$	Sigma
Hydrogen peroxide solution, 30%, puriss., stabilized	H_2O_2	Sigma-Aldrich
Methyl alcohol, Anhydrous	CH_3OH	Mallinckrodt Chemicals
Cellulose, microcrystalline, powder, 20 μm	$(C_6H_{10}O_5)_n$	Aldrich
D-(+)-Cellobiose, minimum 98%	$C_{12}H_{22}O_{11}$	Sigma-Aldrich
D-(+)-Glucose, minimum 99.5%	$C_6H_{12}O_6$	Sigma
D-(-)-Fructose, minimum 99%	$C_6H_{12}O_6$	Sigma
1-Ehtyl-3-methylimidazolium chloride, 98%	$C_6H_{11}ClN_2$	Aldrich

Acetonitrile	C_2H_3N	J. T. Baker
Sulfuric acid	H_2SO_4	Shimakyu's pure chemicals
1,6-Anhydro-beta-D-glucopyranose, 99%	$C_6H_{10}O_5$	Alfa Aesar
5-hydroxymethyl-2-furaldehyde, 98+%	$C_6H_6O_3$	Alfa Aesar
Crystal violet	$C_{25}N_3H_{30}Cl$	Sigma
Fast Garnet GBC base	$C_{14}H_{15}N_3$	Sigma-Aldrich
Methyl red	$C_{15}H_{15}N_3O_2$	-
Neutral red	$C_{15}H_{17}ClN_4$	-
Phenol red	$C_{19}H_{14}O_5S$	Sigma-Aldrich
Phenolphthalein	$C_{20}H_{14}O_4$	-
2,4-Dinitroanline	$C_6H_5N_3O_4$	-

3.2 Experimental apparatuses

3.2-1 Solid state Nuclear Magnetic Resonance (NMR)

The functional groups on LPMSNs materials were examined by solid state NMR (Bruker DSX-400WB NMR spectrometer, NMR/Solid 400).

3.2-2 Nitrogen Adsorption/Desorption Isotherm

The porous properties of LPMSNs were analyzed using nitrogen adsorption/desorption isotherms on a Micromeritics ASAP 2000 instrument at 77 K. The specific surface area and pore size distribution were calculated using the method of Brumauer-Emmett-Teller (BET) and Barrett-Joyner-Halenda (BJH).

3.2-3 Field Emission Scanning Electron Microscope (SEM)

The morphology and particles sizes of the LPMSN, LPMSN-NH_2, LPMSN-SO_3H and LPMSN-Both were observed with SEM (NovaTM Nano SEM).

3.2-4 X-ray Diffractometer (XRD)

The crystallinity of cellulose was analyzed by powder X-ray diffraction on a Rigaku Ultima IV with Cu Kα (40 kV, 40 mA).

3.2-5 High Performance Liquid Chromatography (HPLC)

The samples were analyzed using high performance liquid chromatography (Jasco, RI-2031) equipped with a Bio-Rad HPX-87H column.

3.3 Experimental methods

3.3-1 Synthesis of ultra large pore mesoporous silica nanoparticles

Mesoporous silica nanoparticles with ultra-large pores were synthesized by modifying a published procedure [17]. Typically, 6.92 ml of Brij-97 was added to 180 ml of deionized water with stirring at room temperature. After Brij-97 totally dissolved, 0.3 ml of (3-aminopropyl)trimethoxysilane (APTMS) and 0.08 ml of dimethyl phthalate (DOP) were added to the Brij-97 aqueous solution. After stirring for 30 min, 6.7 ml of tetraethyl orthosilicate (TEOS) was added to the mixture of APTMS/DOP/Brij-97 solution, and the mixture was stirred at room temperature for 24 h, followed by heating at 100 ºC for 24 h. Finally, the white precipitate was collected by filtration, washed with methanol and water several times in order to remove the Brij-97, and dried in lyophilizer. The resulting sample was called as ultra large pore mesoporous silica nanoparticles (LPMSN).

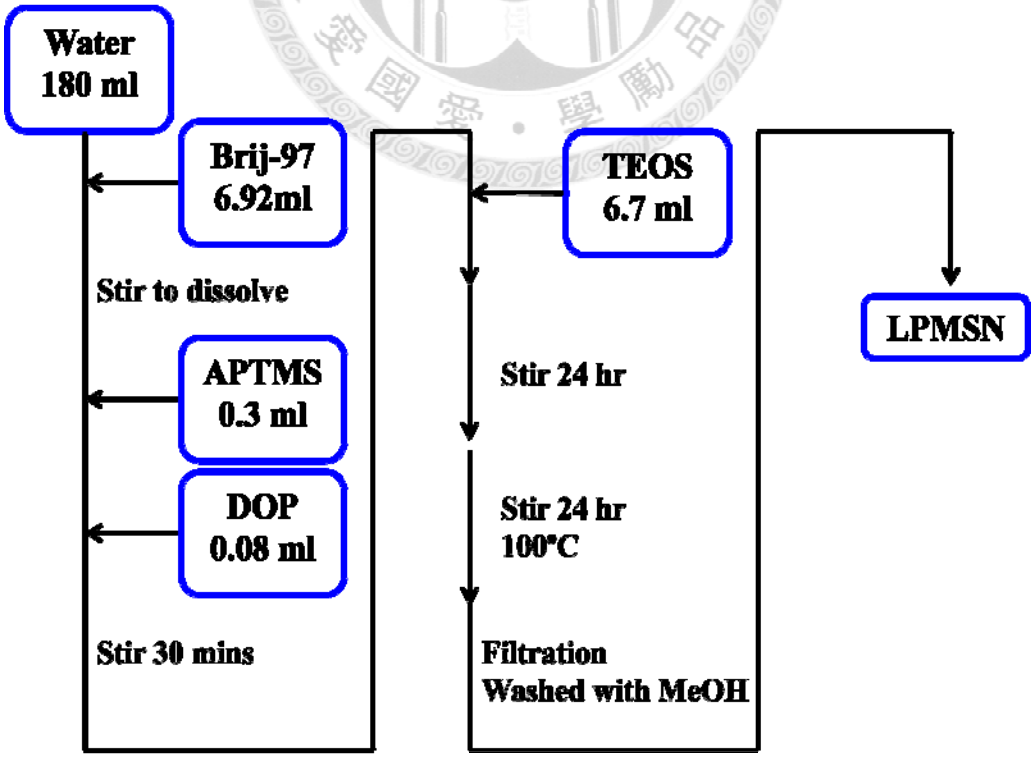

Figure 3.3-1 Flow chart of synthesis of LPMSN

3.3-2 Functionalization of LPMSN into different kinds of catalyst

To synthesize LPMSN with different functionality, the organosilane (APTMS and MPTMS) was grafted onto the surface of LPMSN. Typically, 1 g of LPMSN in the 100 ml two-neck round-bottom flask was degassed in vacuum system at 110 ºC for 3 h. After that, 40 ml of toluene was injected into the flask under nitrogen containing base, followed by injecting organosilanes. The amount of organosilane was calculated by the amount of silanol group on the LPSMN (~6 mmol/g LPMSN). Then, the mixture was heated and refluxed at 110 ºC for 24 h. Finally, the as-synthesized LPMSN was collected by filtration, washed with toluene several times in order to remove the residual reactant, and dried in lyophilizer. The resulting samples were called LPMSN-NH_2 and LPMSN-SH.

LPMSN-SH also immersed in the mercaptopropionic aicd to control the acid strength into different order.

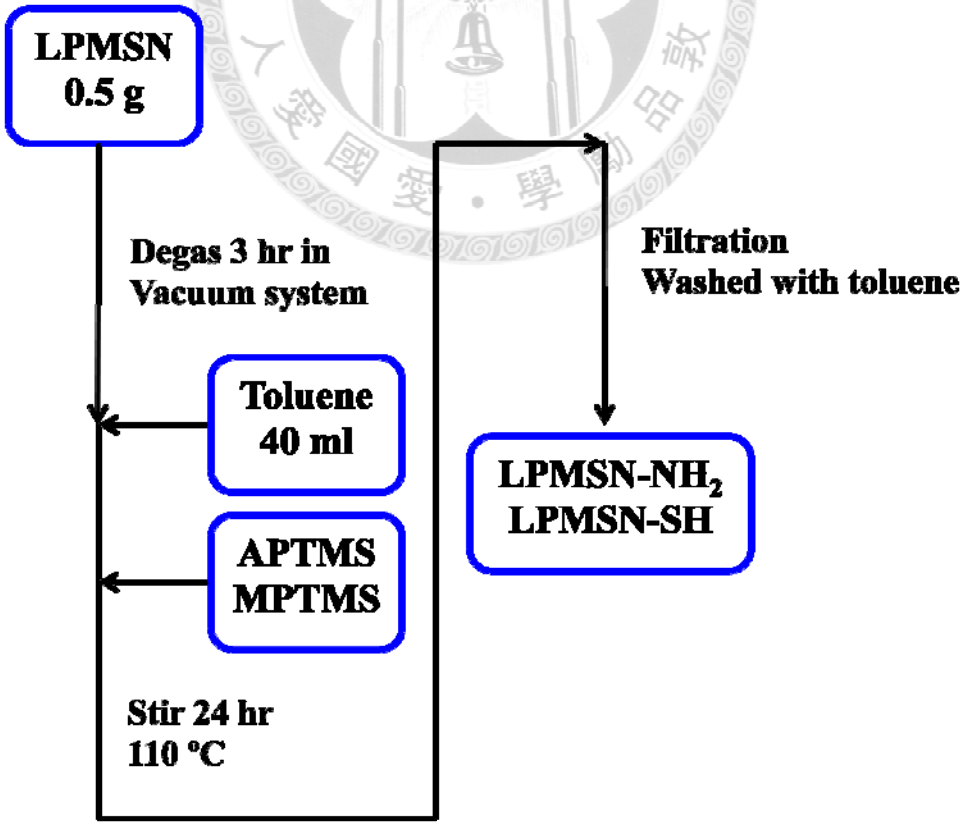

Figure 3.3-2 Flow chart of synthesis of functionalized LPMSN

3.3-3 Oxidization of LPMSN-SH into LPMSN-SO_3H

The oxidation of LPMSN-SH into LPMSN-SO_3H was oxidized by modifying a published procedure [46]. Typically, 0.5 g of LPMSN-SH was added to the mixture of 10 ml hydrogen peroxide, 10ml deionized water, and 10 ml methanol. The mixture was stirred at room temperature for overnight. After that, the resulting precipitate was collected by filtration, washed with deionized water several times and dried in lyophilizer. The resulting sample was called LPMSN-SO_3H.

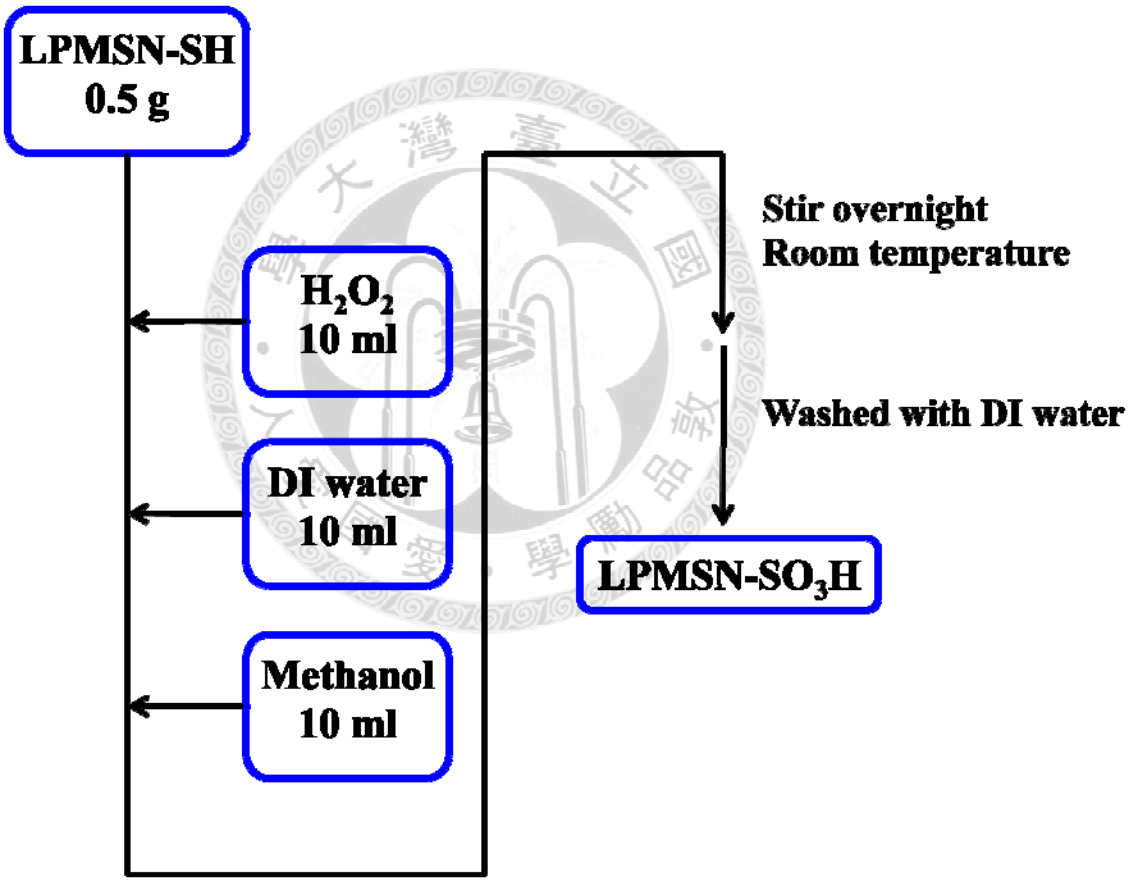

Figure 3.3-3 Flow chart of oxidation of LPMSN-SH

3.3-4 Synthesis of the bi-functionalized catalyst

Step 3.3-2 was repeated while LPMSN was replaced by LPMSN-SO_3H. The final product was called bi-functionalized mesoporous silica nanoparticles (LPMSN-Both).

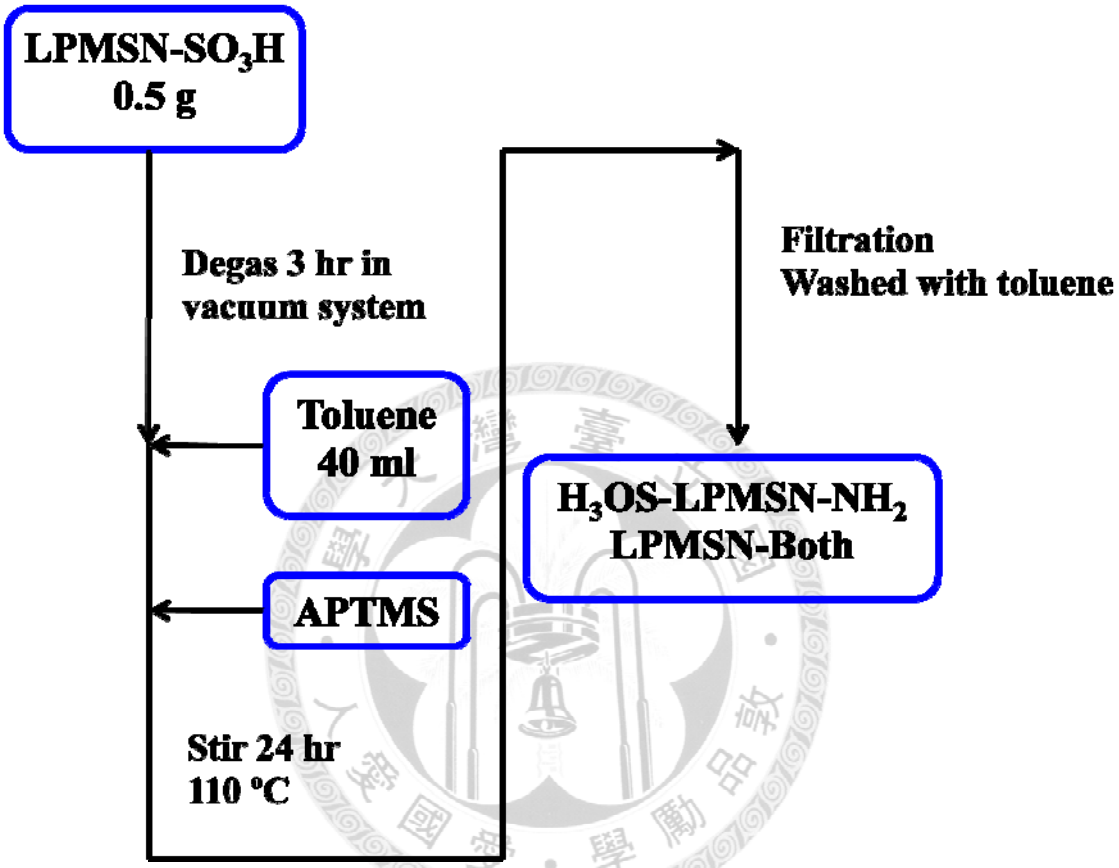

Figure 3.3-4 Flow chart of synthesis of LPMSN-Both

3.3-5 Characterization of acid strength of the different catalysts

The acid strength was measured by modifying a published procedure [47]. Typically, several drops of 0.1 wt% indicator $_{(aq)}$ were added to 10 mg of samples (LPMSN, LPMSN-NH_2, LPMSN-SO_3H and LPMSN-Both). After that, observed the color change of these samples to judge the acid strength of each different catalyst. All of indicators we used in this study was shown in the **Table 3.3-5**.

Table 3.3-5 Different kinds of indicator

Indicator	Color alkaline form	Color acid form	pKa value
Crystal violet	Blue	Yellow	+0.8
Fast Garnet GBC base	Yellow	Red	+2
Methyl red	Yellow	Red	+4.8
Neutral red	Yellow	Red	+6.8
Phenol red	Red	Yellow	+7.65
Phenolphthalein	Red	Colorless	+9.3
2,4-Dinitroaniline	Violet	Yellow	+15

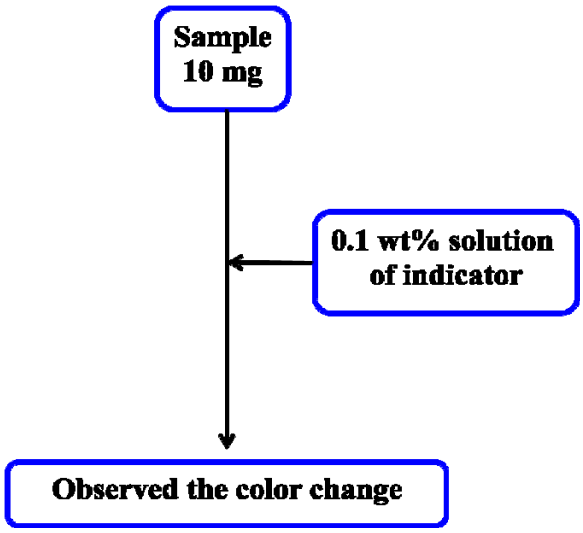

Figure 3.3-5 Flow chart of SOP of acid strength

3.3-6 Preparation of ionic liquid

If ionic liquid contained too much water, it will lower the ability of cellulose pretreatment. It is why ionic liquid needed to separate into small vials.

Typically, we needed to prepare several spoons, 20 ml vials and ionic liquids and put all of these things into the glove bag. Then, sealed the glove bag and linked to the nitrogen gas cylinder. In order to dilute the moisture in the glove bag we needed to fill and vent nitrogen gas for several times. After that, we could start to separate ionic liquid into 20 ml vials.

3.3-7 Lignocellulosic conversion

3.3-7a Cellulose conversion

The cellulosic conversion includes two major parts pretreatment and reaction. The pretreatment for cellulose dissolution was performed by adding 15 mg of cellulose into 150 µl of 1-ethyl-3-methylimidazolium chloride and heating the mixture at 120 ºC for 0.5 h with stirring. Typically, 4 mg of as-synthesized catalyst and 16.67 µl of DI water were added to the cellulose/[EMIM]Cl solution.

This reaction was also carried out at 120 ºC for 3 h. After that, the catalysts were filtrated using a syringe filter, and then the solution were analyzed using a high-performance liquid chromatography (Jasco, RI-2031) equipped with a Bio-Rad HPX-87H column.

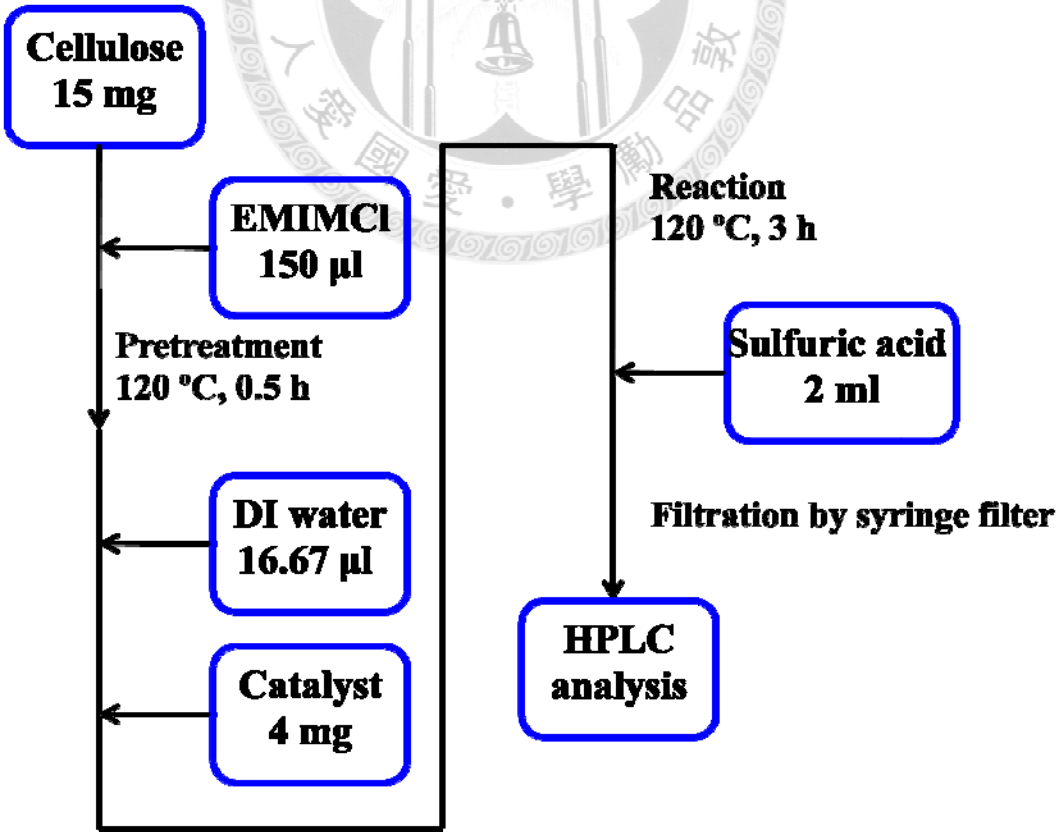

Figure 3.3-7a Flow chart of SOP of cellulosic conversion

3.3-7b Cellobiose conversion

The SOP of conversion of cellobiose was similar to cellulose except the pretreatment step. Typically, 15 mg of cellobiose, 16.67μl of DI water and 4 mg of as-synthesized catalyst were added into 150 μl of [EMIM]Cl and heating the mixture at 120 ℃ for 3 h. After that, the catalysts were filtrated using a syringe filter, and then the solution were analyzed by HPLC.

3.3-7c Glucose and fructose conversion

The SOP of conversion of glucose and fructose were similar to cellobiose. But there was no hydrolysis step in this section, the addition of DI water was removed.

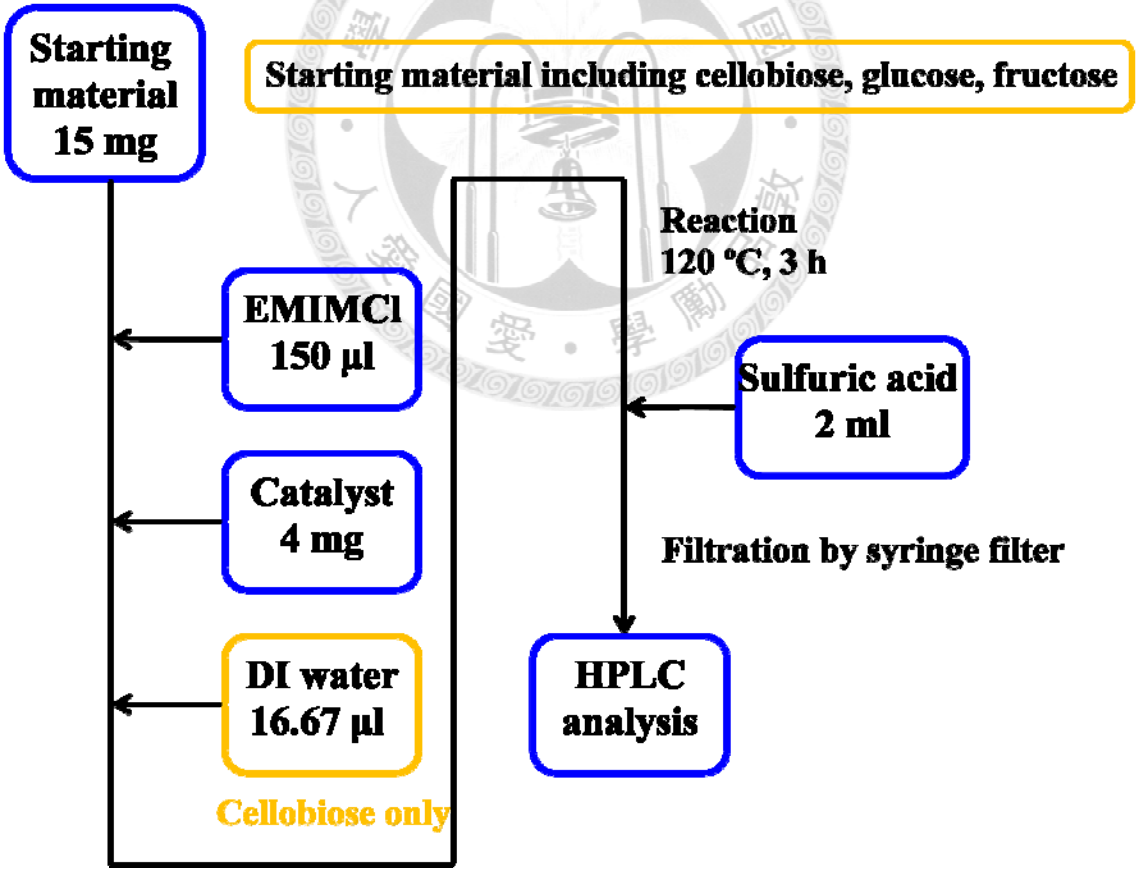

Figure 3.3-7b Flow chart of SOP of cellobiose, glucose and fructose conversion

Chapter 4 Results and discussion

There are two parts to discuss in this section. First is the characterization of different ultra large pore silica nanoparticles (LPMSN, LPMSN-NH_2, LPMSN-SO_3H and LPMSN-Both). Second is the application of these catalysts in the lignocellulosic conversion.

4.1 Characterization of as-synthesized LPMSNs

4.1-1 Morphology of as-synthesized LPMSNs

The morphology of the ultra large pore mesoporous silica nanoparticles were shown in **Figure 4.1-1a and 4.1-1b**. The SEM images showed the uniform and spherical morphology for LPMSN with particles sizes of approximately 500-600 nm, respectively. The other as-synthesized LPMSN (LPMSN-NH_2, LPMSN-SO_3H and LPMSN-Both) were also shown in **Figure 4.1-1c, 4.1-1d, 4.1-1e, 4.1-1f, 4.1-1g and 4.1-1h**. The SEM images show they are spherical morphology with particle sizes of 500-600 nm. Although there were some small particles around LPMSN, these particles were formed from the hydrolysis of silane (APTMS or MPTMS).

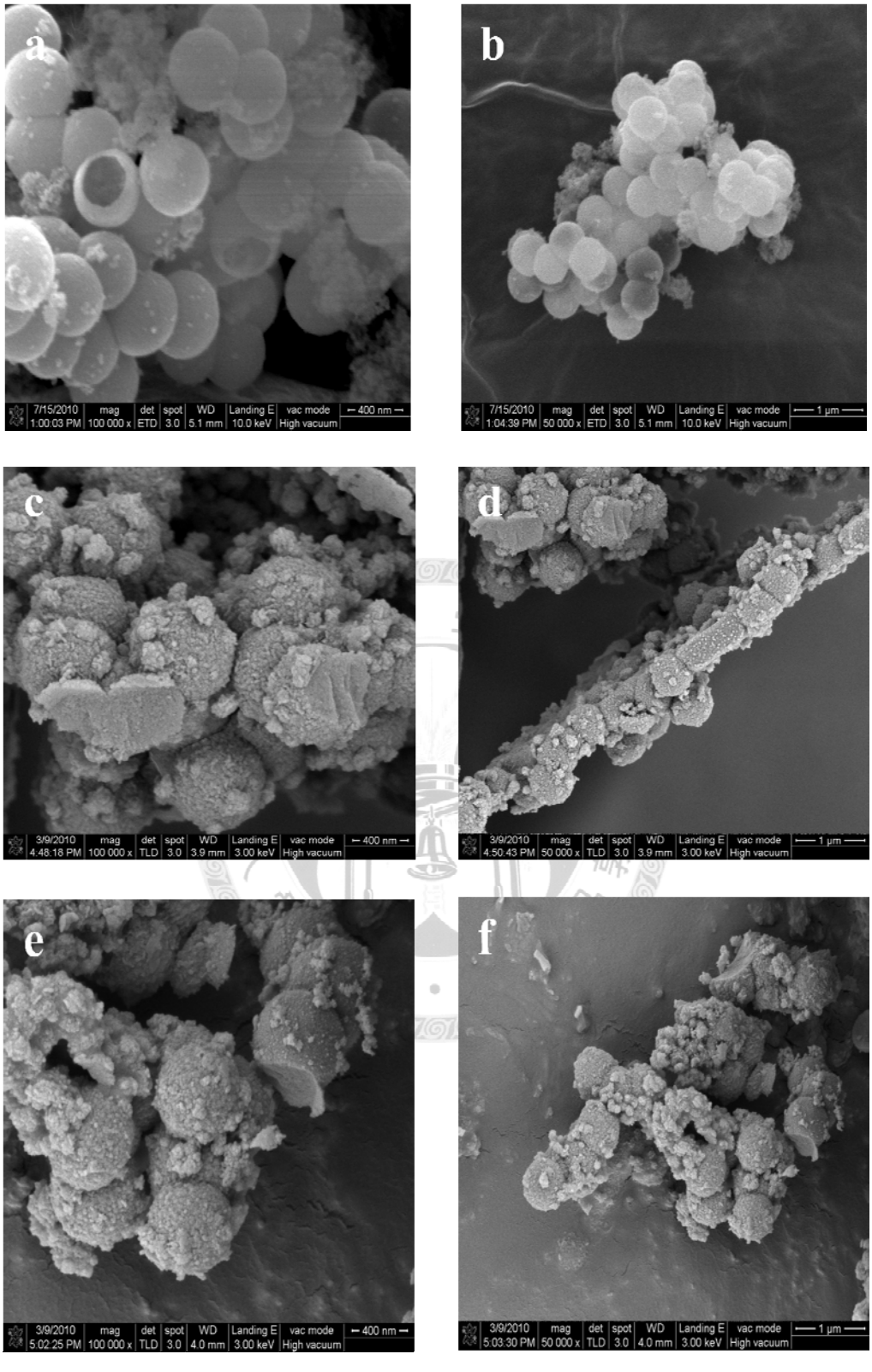
a
7/15/2010 | mag | det | spot | WD | Landing E | vac mode | 400 nm
1:00:03 PM | 100 000 x | ETD | 3.0 | 5.1 mm | 10.0 keV | High vacuum
b
7/15/2010 | mag | det | spot | WD | Landing E | vac mode | 1 µm
1:04:39 PM | 50 000 x | ETD | 3.0 | 5.1 mm | 10.0 keV | High vacuum
c
3/9/2010 | mag | det | spot | WD | Landing E | vac mode | 400 nm
4:48:18 PM | 100 000 x | TLD | 3.0 | 3.9 mm | 3.00 keV | High vacuum
d
3/9/2010 | mag | det | spot | WD | Landing E | vac mode | 1 µm
4:50:43 PM | 50 000 x | TLD | 3.0 | 3.9 mm | 3.00 keV | High vacuum
e
3/9/2010 | mag | det | spot | WD | Landing E | vac mode | 400 nm
5:02:25 PM | 100 000 x | TLD | 3.0 | 4.0 mm | 3.00 keV | High vacuum
f
3/9/2010 | mag | det | spot | WD | Landing E | vac mode | 1 µm
5:03:30 PM | 50 000 x | TLD | 3.0 | 4.0 mm | 3.00 keV | High vacuum

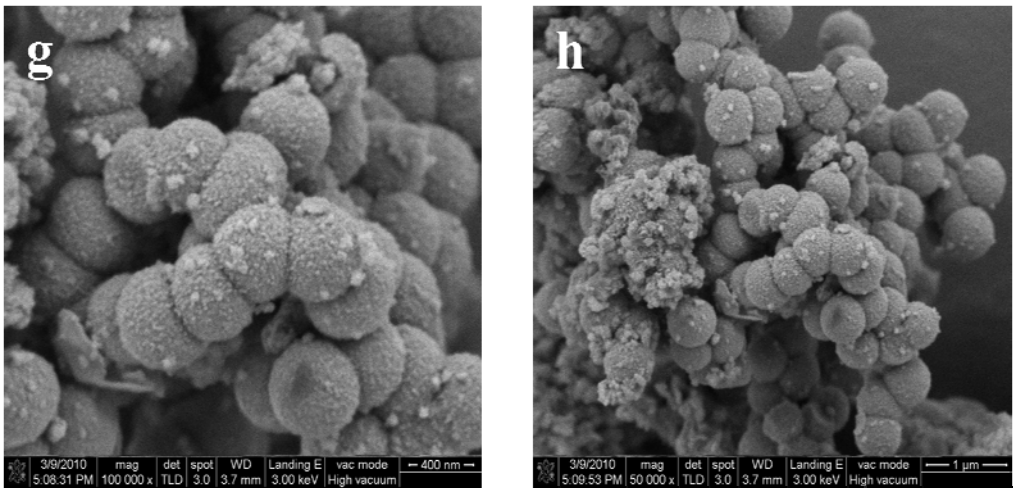

Figure 4.1-1 Morphology of LPMSN, LPMSN-NH_2, LPMSN-SO_3H and LPMSN-Both a LPMSN (400 nm), b LPMSN (1 μm), c LPMSN-NH_2 (400 nm), d LPMSN-NH_2 (1 μm), e LPMSN-SO_3H (400 nm), f LPMSN-SO_3H (1 μm), g LPMSN-Both (400 nm), h LPMSN-Both (1 μm).

4.1-2 Porous properties of as-synthesized LPMSNs

All of the LPMSN, LPMSN-NH_2, LPMSN-SO_3H and LPMSN-Both exhibited type IV nitrogen adsorption/desorption isotherms as shown in **Figure 4.1-2a, 4.1-2b, 4.1-2c and 4.1-2d**, representing an adsorption on mesoporous solids. The adsorption at low relative pressures was similar to type III (macroporous solid). While the nitrogen adsorption amount increased at high relative pressure because of the capillary condensation in mesopores. There exhibited a hysteresis loop for all of as-synthesized LPMSN. The BET specific surface areas for LPMSN, LPMSN-NH_2, LPMSN-SO_3H and LPMSN-Both were 233.24, 166.32, 169.85 and 62.97 m^2/g, respectively. The specific surface area of LPMSN-NH_2 and LPMSN-SO_3H are smaller than LPMSN, because both of them were grafted silane for once. After grafting, there were many surface area will be occupied resulting the smaller specific surface area. The specific surface area of LPMSN-Both was the smallest due to it was grafted for twice. The BJH pore size distribution for LPMSN, LPMSN-NH_2, LPMSN-SO_3H and LPMSN-Both were 42.12, 32.21, 28.09 and 26.71 nm. As the same reasons while grafting once or twice the pore size will be smaller than the previous one. All the data of BET specific surface area and BJH pore size distribution were summarized in **Table 4.1-2**.

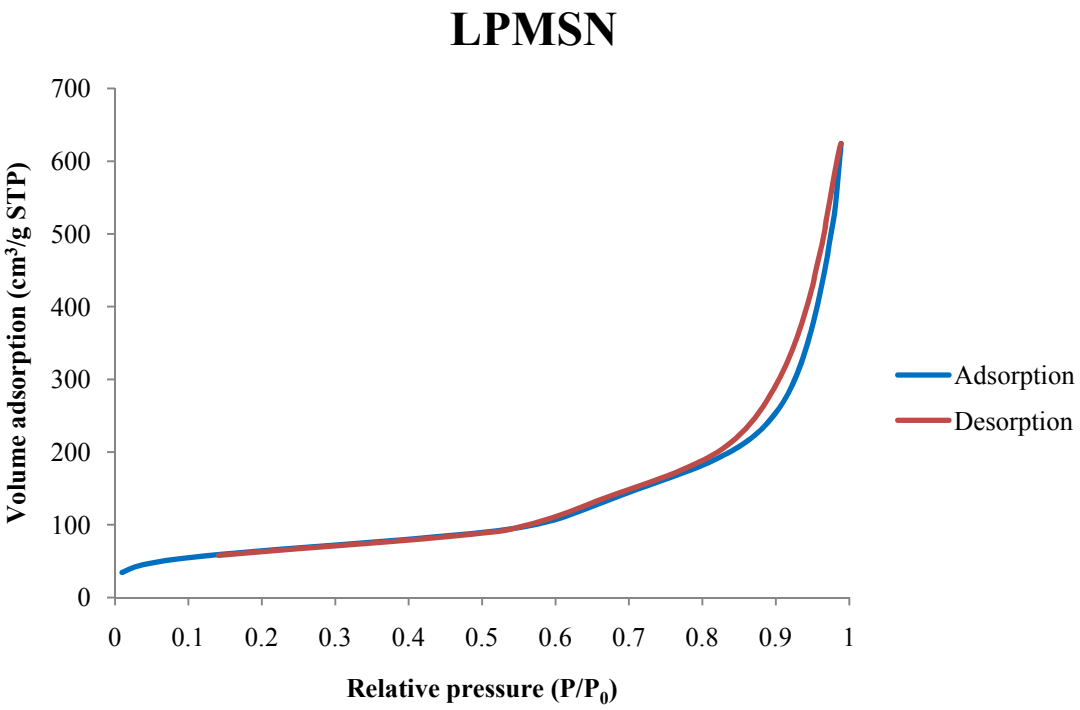

Figure 4.1-2a Nitrogen adsorption/desorption isotherm of LPMSN

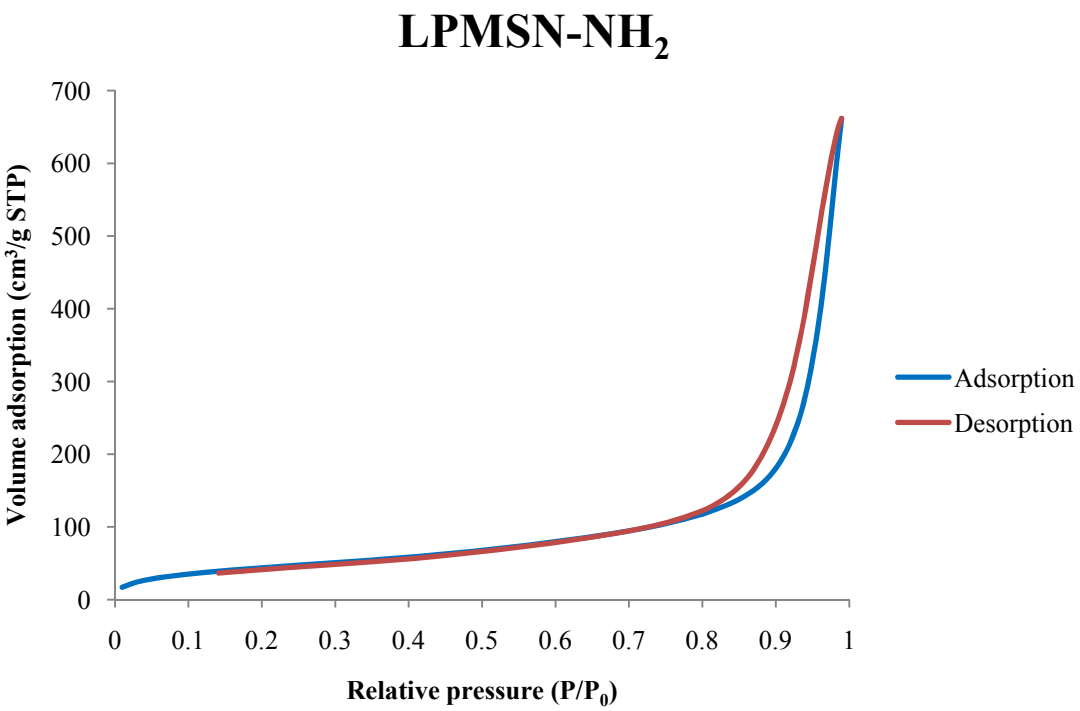

Figure 4.1-2b Nitrogen adsorption/desorption isotherm of LPMSN-NH_2

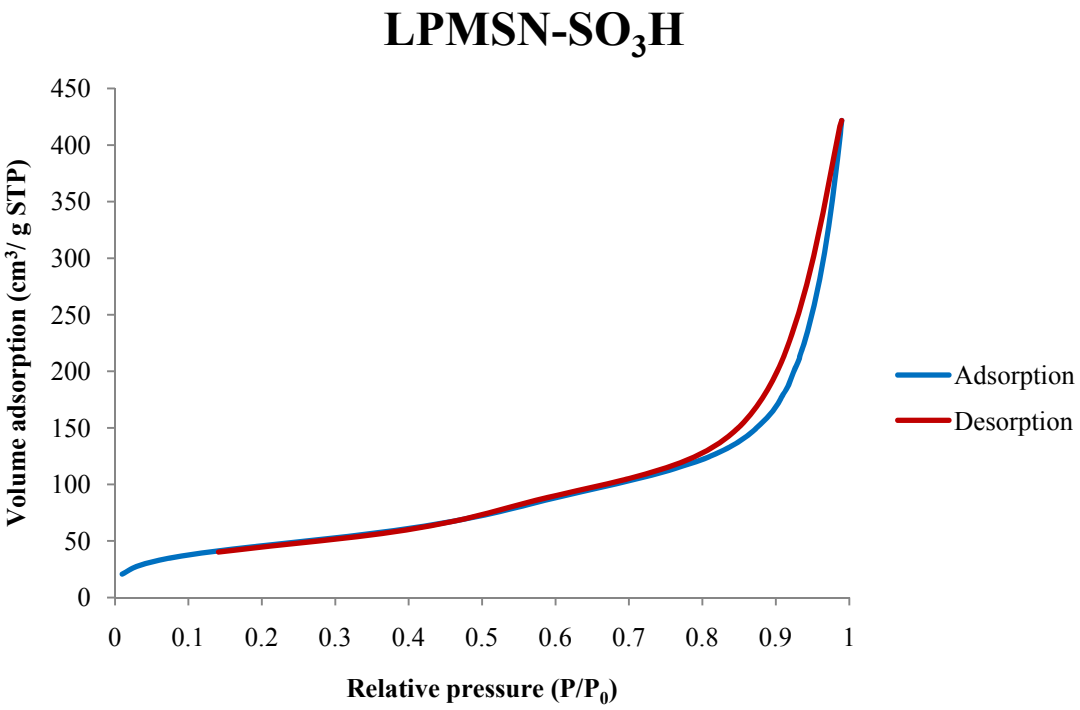

Figure 4.1-2c Nitrogen adsorption/desorption isotherm of LPMSN-SO_3H

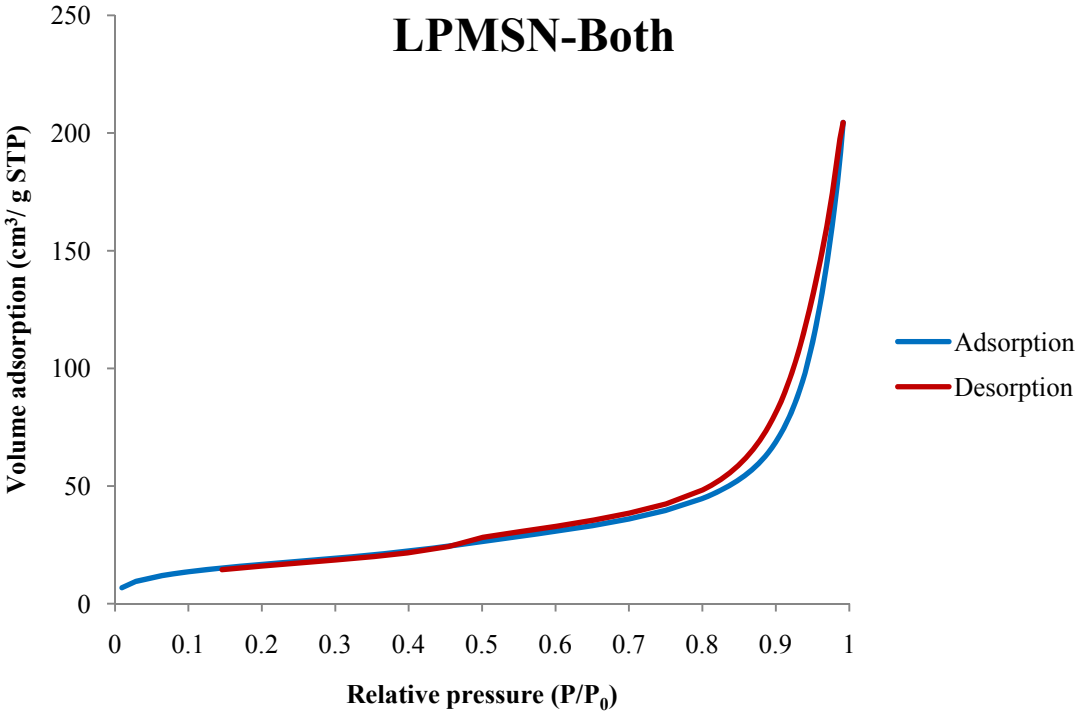

Figure 4.1-2d Nitrogen adsorption/desorption isotherm of LPMSN-Both

Table 4.1-2 Summary of specific surface area and pore size distribution of LPMSN, LPMSN-NH_2, LPMSN-SO_3H and LPMSN-Both

Name	**BET** **specific surface area**	**BJH** **pore size distribution**
LPMSN	233.24 m^2/g	42.12 nm
LPMSN-NH_2	166.32 m^2/g	32.21 nm
LPMSN-SO_3H	169.85 m^2/g	28.09 nm
LPMSN-Both	62.97 m^2/g	26.71 nm

4.1-3 Functionalization of as-synthesized LPMSNs

This study qualitatively and quantitatively investigated the functional groups on the LPMSN using ^{13}C and ^{29}Si CPMAS solid state nuclear magnetic resonance (NMR). As shown in **Figure 4.1-3a**, there were three distinct peaks at approximately 11, 22 and 42 ppm corresponding to the carbons on the Si-CH_2-CH_2-CH_2-NH_2 from left to right [48]. This result indicating the amine group were grafted onto the LPMSN surface and exhibit the functionality of alkaline. In **Figure 4.1-3b**, the three individual peaks at 11, 18 and 54 ppm also corresponding to the carbons on the Si-CH_2-CH_2-CH_2-SO_3H from left to right [49]. This data proved that the sulfonic group were grafted onto the LPMSN surface and exhibited the functionality of acid. This result also exhibited the peak of incomplete oxidation of thiol group. Besides that, the peaks of amine group were shown here. The reason was while synthesizing LPMSN, APTMS was added in order to control the pore size. In both figures have the peak at 71 ppm due to the surfactant (Brij 97) wasn't totally removed in extraction step. The amount of functional and hydroxyl group were listed in **Table 4.1-3a**. The amount of silanol group of LPMSN, LPMSN-NH_2, LPMSN-SO_3H and LPMSN-Both are 6.12, 7.28, 5.14 and 2.51 mmol/g LPMSN. The amount of functional group of LPMSN, LPMSN-NH_2, LPMSN-SO_3H and LPMSN-Both are 1.06, 1.67, 1.35 and 2.32 mmol/g LPMSN. The incorporation and loading amount of functional group onto the LPMSN could be identified and calculated by CPMAS ^{29}Si NMR. As shown in **Figure 4.1-3c, 4.1-3d, 4.1-3e and 4.1-3f**, there were five individual peaks corresponding to Q^4 ($Si(OSi)_4$), Q^3 ($Si(OSi)_3OH$), Q^2 ($Si(OSi)_2(OH)_2$), T^3 ($RSi(OSi)_3$) and T^2 ($RSi(OSi)_2OH$). So the presence of T^2 and T^3 were also the evidence to prove both amine and sulfonic group are on the LPMSN. The percentage of Q^4, Q^3, Q^2, T^3 and T^2 were summarized in **Table 4.1-3b**.

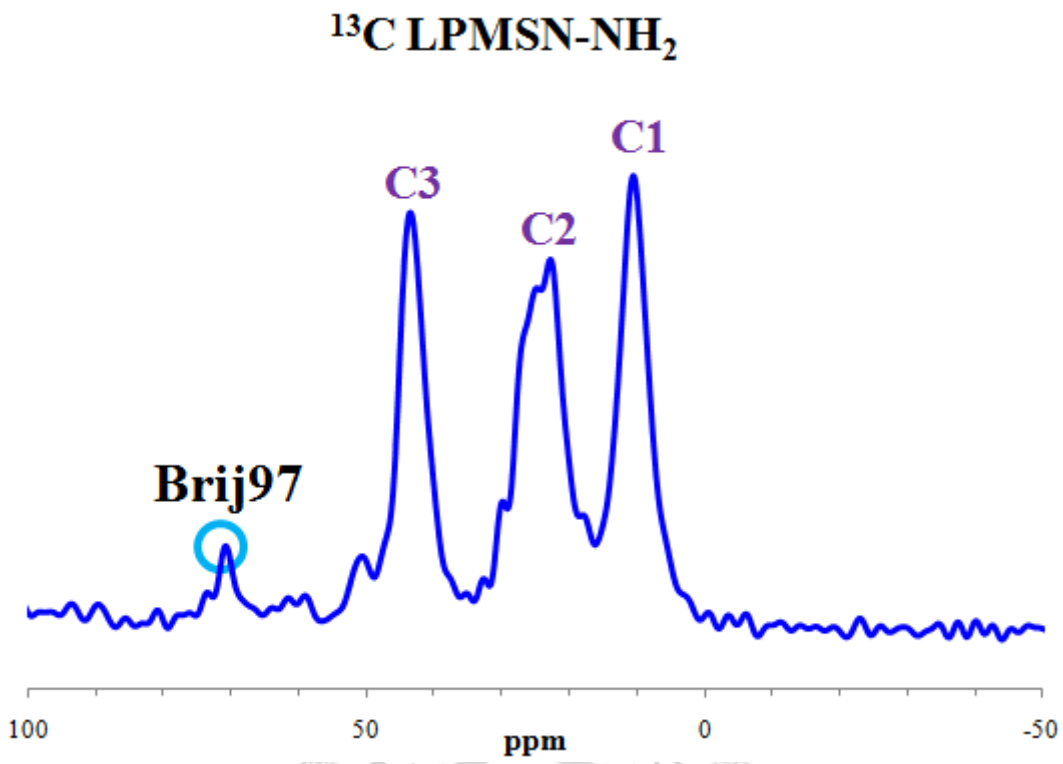

Figure 4.1-3a Solid state NMR ^{13}C spectrum of LPMSN-NH_2

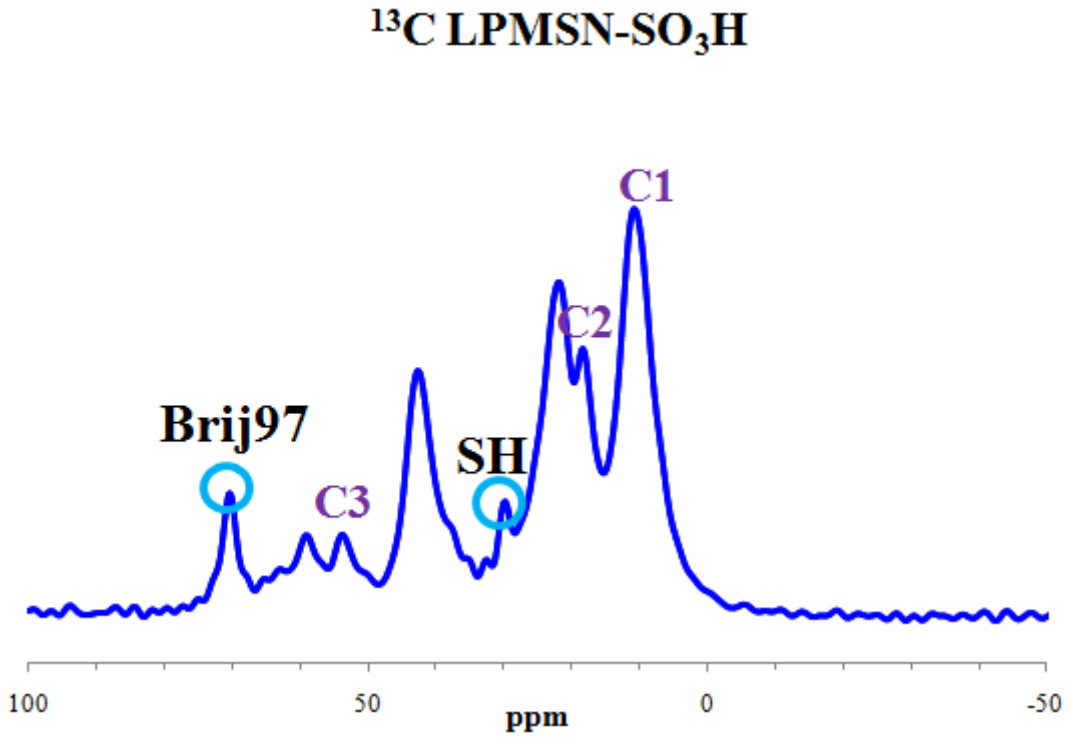

Figure 4.1-3b Solid state NMR ^{13}C spectrum of LPMSN-SO_3H

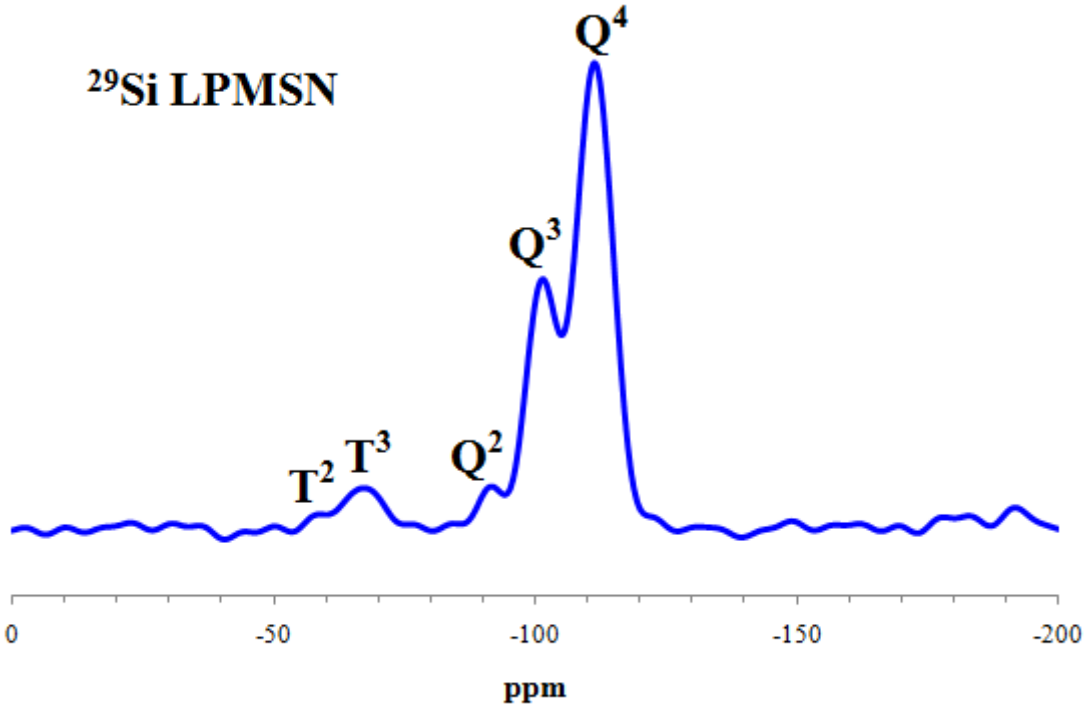

Figure 4.1-3c Solid state NMR ^{29}Si spectrum of LPMSN

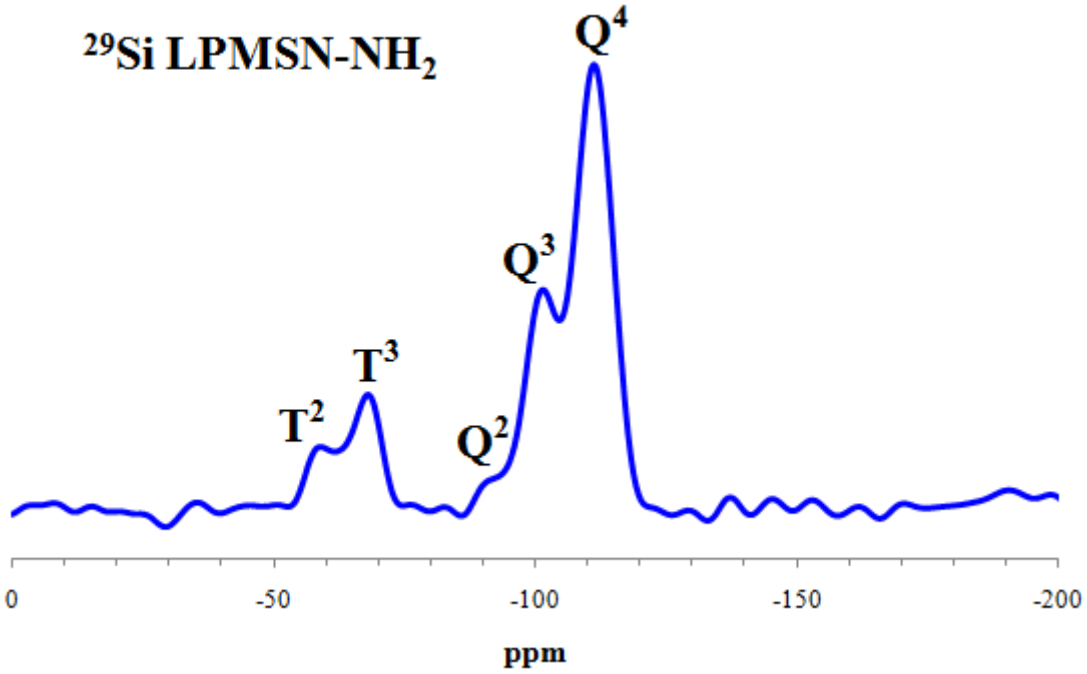

Figure 4.1-3d Solid state NMR ^{29}Si spectrum of LPMSN-NH_2

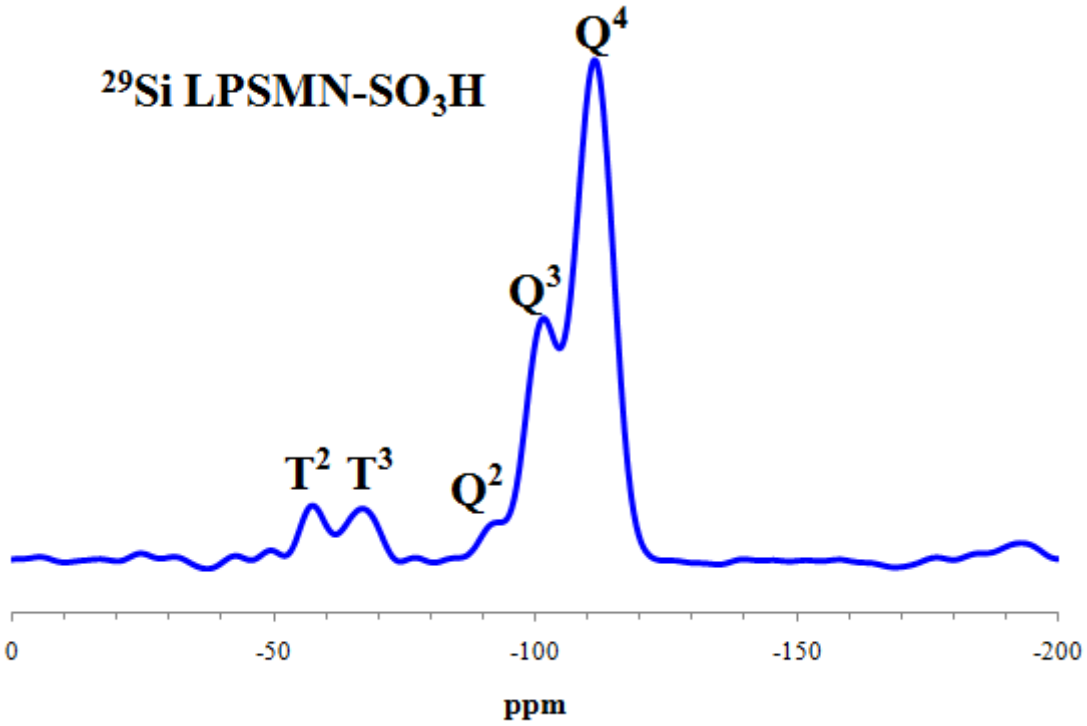

Figure 4.1-3e Solid state NMR ^{29}Si spectrum of LPMSN-SO_3H

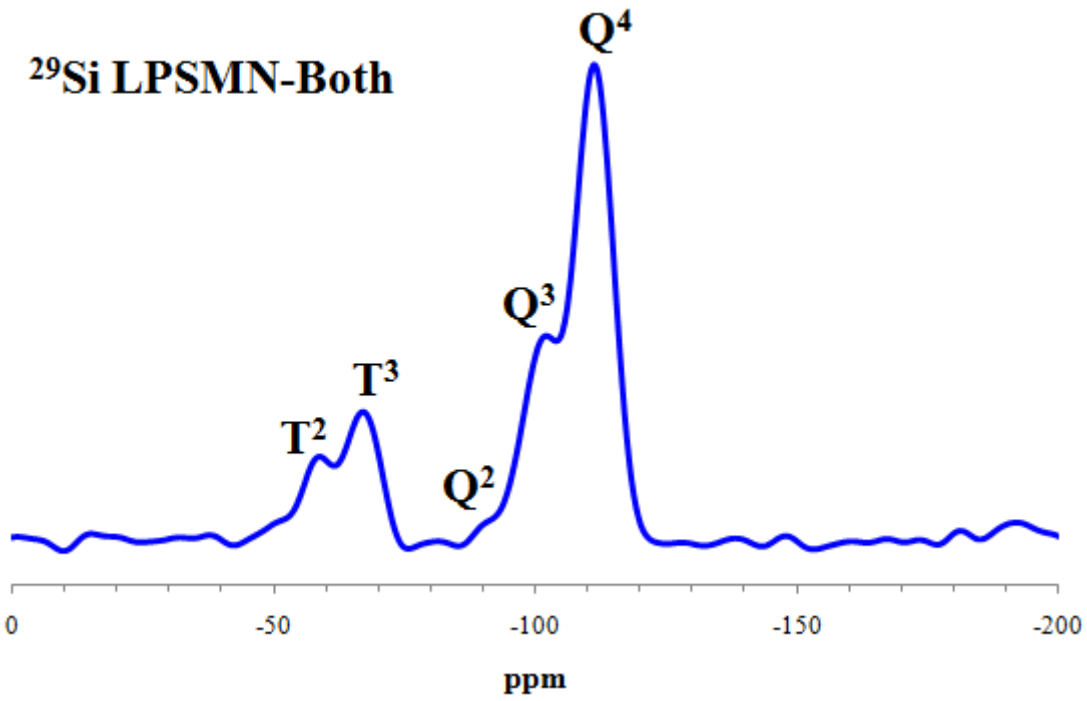

Figure 4.1-3f Solid state NMR ^{29}Si spectrum of LPMSN-Both

Table 4.1-3a Functional and silanol group on the LPMSN, LPMSN-NH_2, LPMSN-SO_3H and LPMSN-Both

Name	Hydroxyl group (mmol/g)	Functional group (mmol/g)
LPMSN	6.12	1.06
LPMSN-NH_2	7.28	1.67
LPMSN-SO_3H	5.14	1.35
LPMSN-Both	2.51	2.32

Table 4.1-3b Percentage of each characteristic peak of ^{29}Si solid state NMR of LPMSN, LPMSN-NH_2, LPMSN-SO_3H and LPMSN-Both

Sample	Q^4 (%)	Q^3 (%)	Q^2 (%)	T^3 (%)	T^2 (%)
LPMSN	56.86	30.59	5.39	5.17	1.98
LPMSN-NH_2	49.78	24.97	13.38	7.62	4.25
LPMSN-SO_3H	56.58	27.35	5.81	6.18	4.08
LPMSN-Both	50.87	21.33	2.85	15.09	9.85

4.1-4 Acid strength of as-synthesized LPMSNs

The acid strength was measured by modifying a published procedure [47]. The data of acid strength were summarized in **Table 4.1-4**. The LPMSN-SO_3H as acid catalyst exhibits the lowest pKa value because of the sulfonic functional group. Although LPMSN contains slight amine groups on it surface, the Lewis acid was stronger than the amine group. LPMSN also exhibited as acid catalyst. LPMSN-Both was containing more amine group resulted in the lower acid strength than LPMSN and LPMSN-SO_3H. LPMSN-NH_2 contained the most amine groups than LPMSN, so the influence of Lewis acid could be eliminated. LPMSN-NH_2 as alkaline catalyst exhibited the highest pKa value. The order of pKa value of each catalyst was LPMSN-SO_3H < LPMSN < LPMSN-Both < LPMSN-NH_2.

Table 4.1-4 Acid strength of LPMSN, LPMSN-NH_2, LPMSN-SO_3H and LPMSN-Both

Catalyst	Acid strength
LPMSN	2 < pKa < 4.8
LPMSN-NH_2	9.3 < pKa < 15
LPMSN-SO_3H	0.8 < pKa < 2
LPMSN-Both	7.65 < pKa < 9.3

4.2 Lignocellulosic conversion

In lignocellulosic conversion, we proposed the reaction route was shown in **Figure 4.2**. It involved several steps including dissolution of cellulose, hydrolysis of oligomers, isomerization of glucose and dehydration of fructose. Herein we will test the reactivity of these as-synthesized catalysts (LPMSN, LPMSN-NH2, LPMSN-SO3H, and LPMSN-Both) using different starting materials (e.g. cellulose, cellobiose, glucose and fructose).

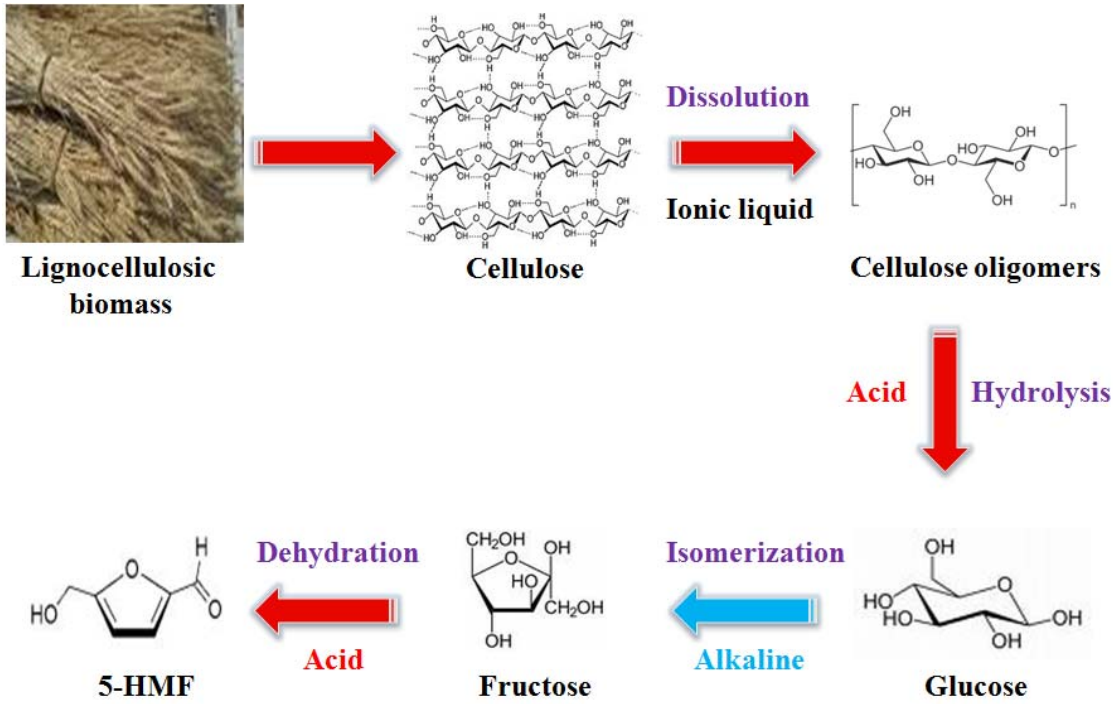

Figure 4.2 Mechanism of lignocellulosic conversion

4.2-1 Definition of yield

Product yield (mol %)

$$Y = \left(\frac{\text{Moles of product}}{\text{Moles of starting materials}} \right) \times 100\ \%$$

All the calculation of final product yield was based on the glucose unit.

4.2-2 Optimal condition of cellulosic conversion

Cellulosic conversion contains multiple and complex reactions, including (1) depolymerization of polysaccharide (cellulose) into glucose with the presence of an acid catalyst; (2) isomerization of glucose into fructose with the presence of an alkaline catalyst; (3) dehydration of fructose into 5-HMF with the presence of an acid catalyst. And the optimal reaction condition of cellulose-to-HMF without adding catalysts such as the dissolution temperature (T_{dis}) and time (t_{dis}) in ILs, the reaction temperature (T_{rxn}) and time (t_{rxn}) and the amount of water were optimized in the previous paper [50]. Here, we adopted our optimized reaction conditions as: cellulose/water = 1/10, T_{dis} = 120 ºC, t_{dis} = 0.5 h, T_{rxn} = 120ºC, t_{rxn} = 3 h for the 1-ethyl-3-imidazolium chloride system.

4.2-3 Destruction of crystalline structure of cellulose in IL

Because cellulose was a crystalline structure, it increased the difficulty of cellulosic conversion and limited the yield of our desired product. It became an important issue to eliminate the crystalline structure of cellulose. In order to make sure the crystalline structure of cellulose before and after IL pretreatment, examined with XRD. As shown in **Figure 4.2-3** the crystalline peak of cellulose at 2θ = 22º disappeared after IL pretreatment (at 120 ºC for 0.5 h in [EMIM]Cl). It proved the crystalline structure was destroyed by ionic liquid ([EMIM]Cl). This result was good for the further cellulosic reaction.

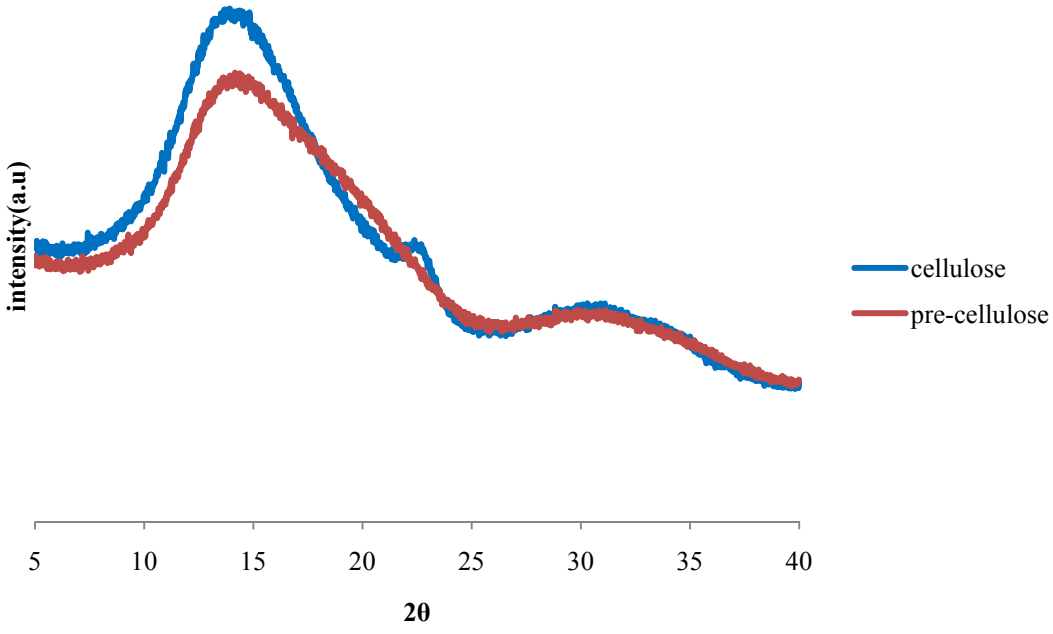

Figure 4.2-3 Crystalline structure of cellulose before and after IL pretreatment

4.2-4 Effect of amount of catalysts in cellulosic conversion

Herein we wanted to apply our synthesized catalysts (LPMSN, LPMSN-NH_2, LPMSN-SO_3H and LPMSN-Both) to cellulosic conversion, the optimal amount of catalyst also needed to be optimized. The effect of different amount of catalysts on the yields of final products converted from cellulose was investigated with the range from 2 to 10 mg using LPMSN-Both as catalyst. The result was shown in **Figure 4.2-4** the best amount of catalyst was carried out with 4 mg of LPMSN-Both. With the presence of 4 mg LPMSN-Both catalysts, it had the largest yields of cellobiose, glucose and 5-HMF. With the increased amount of catalysts, the yields of each product were suddenly dropped down. We suggested it was because the inefficient stir and further decomposition of final products when too many catalysts were added in the reaction mixture.

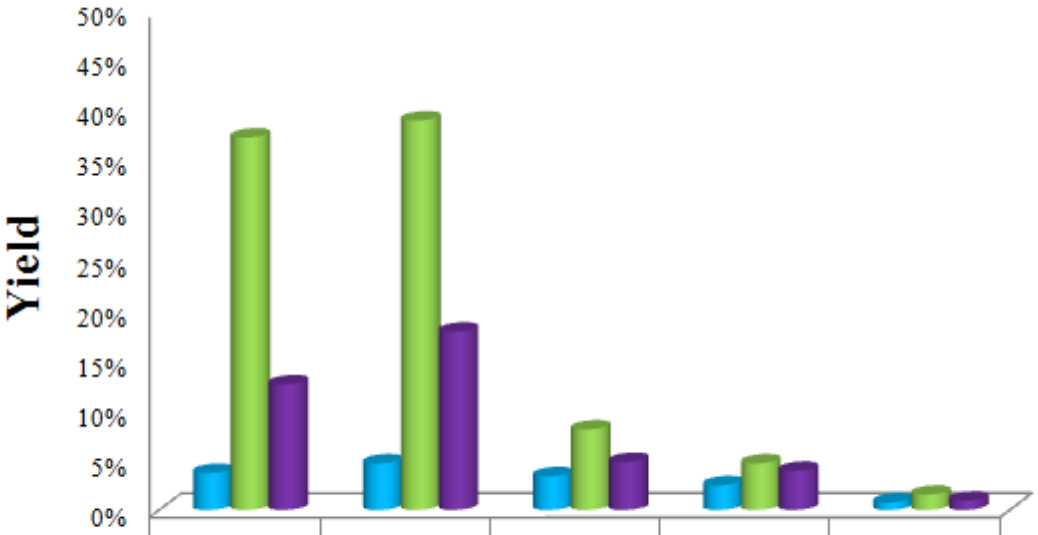

	2 mg	4 mg	6 mg	8 mg	10 mg
cellobiose	3.70%	4.66%	3.38%	2.47%	0.76%
glucose	37.32%	39.01%	8.06%	4.66%	1.52%
5-HMF	12.58%	17.86%	4.80%	3.91%	0.92%

Figure 4.2-4 Optimal amount of catalysts in cellulosic conversion

Based on the optimal condition of cellulose, we adopted this condition to the further small starting materials (e.g. cellobiose, glucose and fructose) to check the catalytic ability of catalysts.

4.2-5 Fructose-to-HMF conversion

While using fructose as starting material, the reaction route of fructose to 5-HMF was via dehydration step was shown in **Figure 4.2-5a**. The reaction condition was fructose = 15 mg, catalyst = 4 mg, T_{rxn} = 120 ºC, t_{rxn} = 3 h in 150 μl of 1-ethyl-3methylimidazolium chloride. The result was shown in **Figure 4.2-5b**, there were no obvious difference between each catalysts, although in this reaction step, fructose needed acid catalyst to dehydrate into 5-HMF. We suggested fructose could be easily converted into 5-HMF in this reaction system because the similar structure between fructose and 5-HMF.

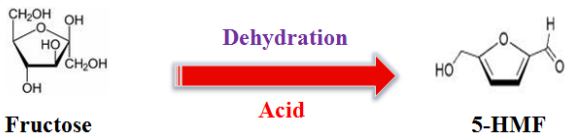

Figure 4.2-5a Reaction route of fructose to 5-HMF

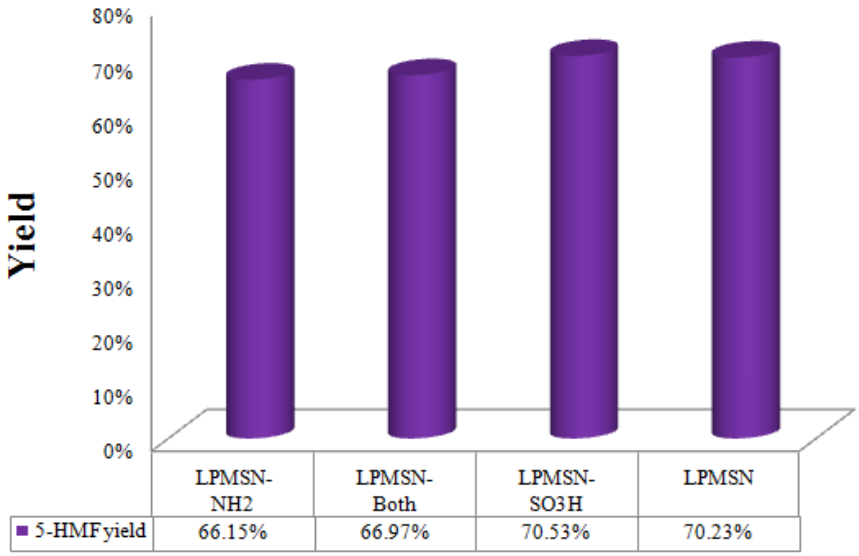

Figure 4.2-5b Fructose-to-HMF conversion

4.2-6 Glucose-to-HMF conversion

The further examination of each catalyst was using glucose as starting materials. In glucose-to-HMF conversion, there involves two reaction routes was shown in **Figure 4.2-6a**. First, the isomerization of glucose needed alkaline catalyst and converted into fructose. Second, the dehydration of fructose needed acid catalyst and converted into 5-HMF. The reaction condition is glucose = 15 mg, catalyst = 4 mg, T_{rxn} = 120 ℃, t_{rxn} = 3 h in 150 μl of 1-ethyl-3methylimidazolium chloride. The result was shown in **Figure 4.2-6b**, when we used alkaline containing catalyst it had the better 5-HMF yields than the others. We propose that was due to the isomerization of glucose was an important step. The more glucose isomerized into fructose, the more yields of 5-HMF. In fructose-to-HMF conversion, we knew that fructose converted into 5-HMF was very easy in this reaction system. So, we assumed the isomerization of glucose was the rate determining step in the synthesis of 5-HMF.

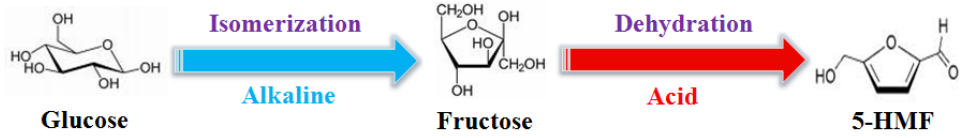

Figure 4.2-6a Reaction route of glucose to 5-HMF

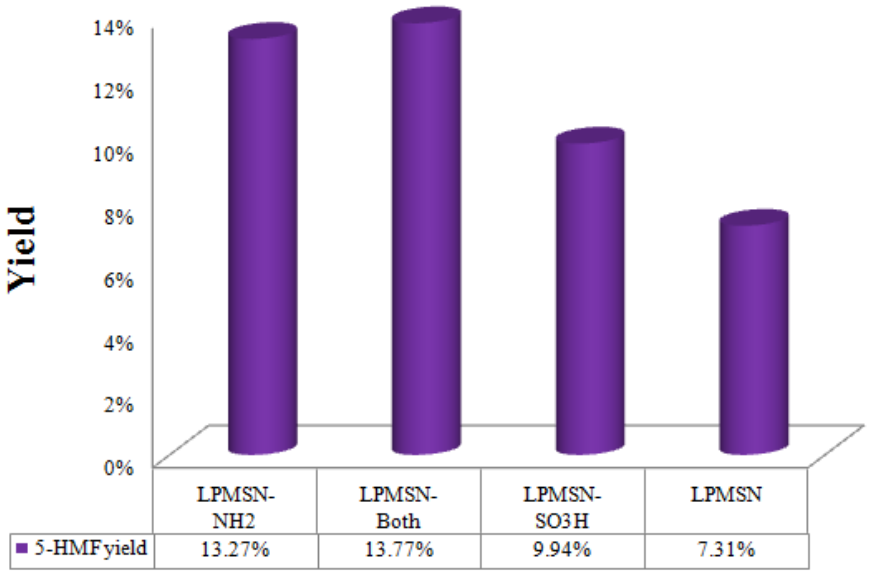

Figure 4.2-6b Glucose-to-HMF conversion

4.2-7 Cellobiose-to-HMF conversion

Herein cellobiose-to-HMF conversion, it involved one more reaction route than glucose-to-HMF conversion was shown in **Figure 4.2-7a**. First, the hydrolysis of cellobiose needed acid catalyst and converted into glucose. Second, the isomerization of glucose needed alkaline catalyst and converted into fructose. Third, the dehydration of fructose needed acid catalyst and converted into 5-HMF. The reaction condition was cellobiose= 15 mg, catalyst = 4 mg, water = 16.67μl, T_{rxn} = 120 ºC, t_{rxn} = 3 h in 150 μl of 1-ethyl-3methylimidazolium chloride. The result was shown in **Figure 4.2-7b**, the best yields of glucose and 5-HMF was carried out while using acid catalyst, LPMSN-SO_3H. The LPMSN also had a good result due to it exhibited as an acid catalyst. We suggest that was because the hydrolysis step was a critical step. The more glucose could be yielded from cellobiose, the more reactant we could get for the further reaction to convert 5-HMF. The yield of glucose was the most abundant using LPMSN-SO_3H catalyst, the other evidence to confirm our assumption. So we proposed the hydrolysis of cellobiose was the rate determining step in the synthesis of 5-HMF.

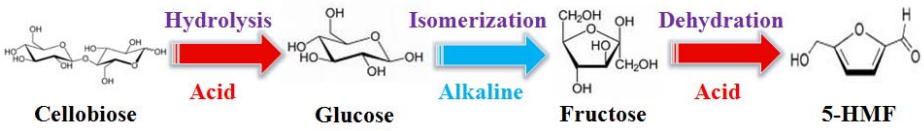

Figure 4.2-7a Reaction route of cellobisoe to 5-HMF

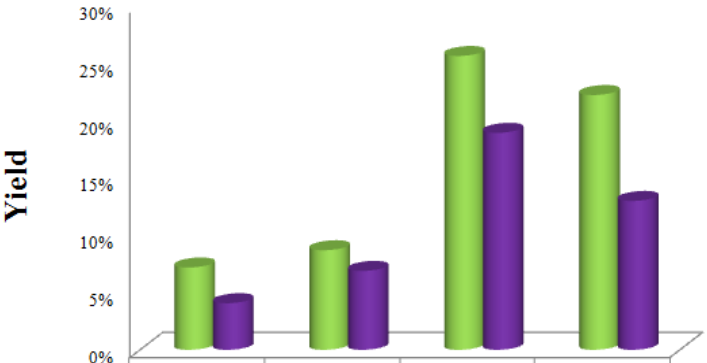

	LPMSN-NH2	LPMSN-Both	LPMSN-SO3H	LPMSN
Glucose yield	7.19%	8.69%	25.63%	22.23%
5-HMF yield	4.07%	6.89%	18.93%	12.99%

Figure 4.2-7b Cellobiose-to-HMF conversion

4.2-8 Cellulose-to-HMF conversion

The most difficult one was cellulose-to-HMF conversion it involved at least three reaction routes. First, the depolymerization and hydrolysis of cellulose needed acid catalyst and converted into disaccharide or oligomers. The further reaction route we assumed it was similar with cellobiose-to-HMF conversion. The reaction condition was cellulose = 15 mg, catalyst = 4 mg, T_{dis} = 120 ºC, t_{dis} = 0.5 h, T_{rxn} = 120ºC, t_{rxn} = 3 h, water = 16.67µl, T_{rxn} = 120 ºC, t_{rxn} = 3 h in 150 µl of 1-ethyl-3methylimidazolium chloride. The result was shown in **Figure 4.2-8b**, although the best yields of 5-HMF was carried out using LPSMN-SO_3H catalyst. The LPMSN-Both catalysts also exhibited a good performance in total yields. So far we were not sure about at which stage will be the dominant step of synthesis of 5-HMF. The detail mechanism of cellulose-to-HMF was still in study.

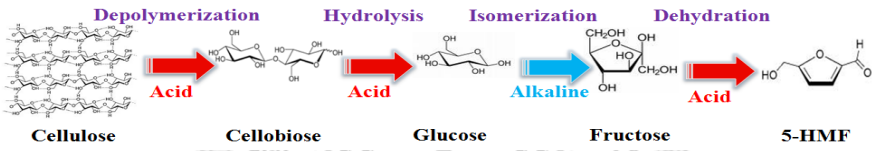

Figure 4.2-8a Reaction route of cellulose to 5-HMF

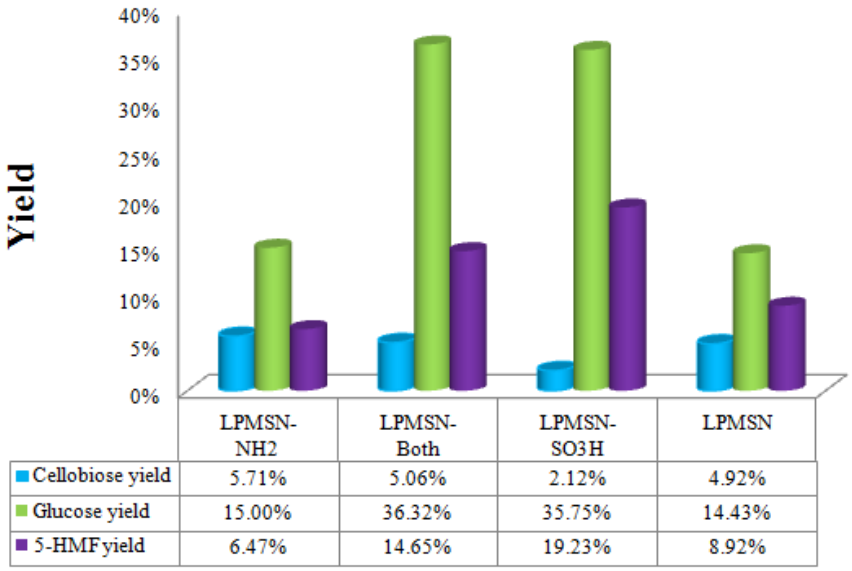

	LPMSN-NH2	LPMSN-Both	LPMSN-SO3H	LPMSN
Cellobiose yield	5.71%	5.06%	2.12%	4.92%
Glucose yield	15.00%	36.32%	35.75%	14.43%
5-HMF yield	6.47%	14.65%	19.23%	8.92%

Figure 4.2-8b Cellulose-to-HMF conversion

Chapter 5 Conclusion

Ultra large pore mesoporous silica nanoparticles (LPMSN) with different functional groups (amine or sulfonic group) have been synthesized and successfully used as solid catalysts for the production of 5-HMF from different starting materials. The morphology, porous properties, acidity and the amount of functional group were characterized. From different starting materials, these catalysts will exhibit different effect on the yields of 5-HMF. In fructose-to-HMF conversion, there are no obvious differences between each catalyst due to fructose is easily dehydrated into 5-HMF. In glucose-to-HMF conversion, the alkaline catalysts could improve the isomerization of glucose and enhance the yield of 5-HMF. In cellobiose-to-HMF conversion, the acid catalysts will enhance the hydrolysis step of cellobiose and yield more 5-HMF than the other catalysts. In cellulose-to-HMF conversion, the acid catalyst (LPMSN-SO_3H) could yield the most amount of 5-HMF. The bi-functioalized catalysts also produce a good yield of total product. Because the cellulose-to-HMF conversion involved too many reaction step, the detail reason we are still in discussion.

Chapter 6 Reference

1. Sing, K.S.W., et al., *Reporting Physisorption Data for Gas Solid Systems with Special Reference to The Determination of Surface-area and Porosity (Recommndations 1984).* Pure and Applied Chemistry, 1985. **57**(4): p. 603-619.
2. De Vos, D.E., et al., *Ordered mesoporous and microporous molecular sieves functionalized with transition metal complexes as catalysts for selective organic transformations.* Chemical Reviews, 2002. **102**(10): p. 3615-3640.
3. Kresge, C.T., et al., *Ordered Mesoporous Molecular-Sieves Synthesized by A Liquid-Crystal Template Mechanism.* Nature, 1992. **359**(6397): p. 710-712.
4. Yanagisawa, T., et al., *The Preparation of Alkyltrimethylammonium-Kanemite Complexes and Their Conversion to Microporous Materials.* Bulletin of the Chemical Society of Japan, 1990. **63**(4): p. 988-992.
5. Soler-illia, G.J.D., et al., *Chemical strategies to design textured materials: From microporous and mesoporous oxides to nanonetworks and hierarchical structures.* Chemical Reviews, 2002. **102**(11): p. 4093-4138.
6. Landry, C.C., et al., *Phase transformations in mesostructured silica/surfactant composites. Mechanisms for change and applications to materials synthesist.* Chemistry of Materials, 2001. **13**(5): p. 1600-1608.
7. Hoffmann, F., et al., *Silica-based mesoporous organic-inorganic hybrid materials.* Angewandte Chemie-International Edition, 2006. **45**(20): p. 3216-3251.
8. Huo, Q.S., et al., *Generalized Synthesis of Periodic Surfactant Inorganic Composite-Materials.* Nature, 1994. **368**(6469): p. 317-321.
9. Zhao, D.Y., et al., *Nonionic triblock and star diblock copolymer and oligomeric surfactant syntheses of highly ordered, hydrothermally stable, mesoporous silica structures.* Journal of the American Chemical Society, 1998. **120**(24): p. 6024-6036.
10. Zhao, D.Y., et al., *Triblock copolymer syntheses of mesoporous silica with periodic 50 to 300 angstrom pores.* Science, 1998. **279**(5350): p. 548-552.
11. Fan, J., et al., *Low-temperature strategy to synthesize highly ordered mesoporous silicas with very large pores.* Journal of the American Chemical Society, 2005.

127(31): p. 10794-10795.

12. Zhao, D.Y., et al., *Ordered mesoporous silicas and carbons with large accessible pores templated from amphiphilic diblock copolymer poly(ethylene oxide)-b-polystyrene.* Journal of the American Chemical Society, 2007. **129**(6): p. 1690-1697.
13. Schmidt-Winkel, P., et al., *Mesocellular siliceous foams with uniformly sized cells and windows.* Journal of the American Chemical Society, 1999. **121**(1): p. 254-255.
14. Schmidt-Winkel, P., et al., *Microemulsion templating of siliceous mesostructured cellular foams with well-defined ultralarge mesopores.* Chemistry of Materials, 2000. **12**(3): p. 686-696.
15. Kim, S.S., T.R. Pauly, and T.J. Pinnavaia, *Non-ionic surfactant assembly of ordered, very large pore molecular sieve silicas from water soluble silicates.* Chemical Communications, 2000(17): p. 1661-1662.
16. Luechinger, M., et al., *The effect of the hydrophobicity of aromatic swelling agents on pore size and shape of mesoporous silicas.* Microporous and Mesoporous Materials, 2005. **79**(1-3): p. 41-52.
17. Chen, L.H., et al., *Novel mesoporous silica spheres with ultra-large pore sizes and their application in protein separation.* Journal of Materials Chemistry, 2009. **19**(14): p. 2013-2017.
18. Stocker, M., *Biofuels and Biomass-To-Liquid Fuels in the Biorefinery: Catalytic Conversion of Lignocellulosic Biomass using Porous Materials.* Angewandte Chemie-International Edition, 2008. **47**(48): p. 9200-9211.
19. Chheda, J.N., Y. Roman-Leshkov, and J.A. Dumesic, *Production of 5-hydroxymethylfurfural and furfural by dehydration of biomass-derived mono- and poly-saccharides.* Green Chemistry, 2007. **9**(4): p. 342-350.
20. Chidambaram, M. and A.T. Bell, *A two-step approach for the catalytic conversion of glucose to 2,5-dimethylfuran in ionic liquids.* Green Chemistry, 2010. **12**(7): p. 1253-1262.
21. Hatanaka, K., et al., *Syntheses of polyesters from 5-hydroxymethyl-2-furfural as a starting material.* Kobunshi Ronbunshu, 2005. **62**(7): p. 316-320.
22. Kroger, M., U. Prusse, and K.D. Vorlop, *A new approach for the production of 2,5-furandicarboxylic acid by in situ oxidation of 5-hydroxymethylfurfural starting from fructose.* Topics in Catalysis, 2000. **13**(3): p. 237-242.

23. Hu, C.W., et al., *A One-Pot Two-Step Approach for the Catalytic Conversion of Glucose into 2,5-Diformylfuran.* Catalysis Letters, 2011. **141**(5): p. 735-741.
24. Tong, X.L., Y. Ma, and Y.D. Li, *Biomass into chemicals: Conversion of sugars to furan derivatives by catalytic processes.* Applied Catalysis a-General, 2010. **385**(1-2): p. 1-13.
25. Antal, M.J.J., W.S.L. Mok, and G.N. Richards, *Mechanisms of Formation of 5-Hydroxymethyl-2-furaldehyde from D-fructose and Sucrose.* Carbohydrate Research, 1990. **119**(1): p. 91-110.
26. Roman-Leshkov, Y., J.N. Chheda, and J.A. Dumesic, *Phase modifiers promote efficient production of hydroxymethylfurfural from fructose.* Science, 2006. **312**(5782): p. 1933-1937.
27. Roman-Leshkov, Y. and J.A. Dumesic, *Solvent Effects on Fructose Dehydration to 5-Hydroxymethylfurfural in Biphasic Systems Saturated with Inorganic Salts.* Topics in Catalysis, 2009. **52**(3): p. 297-303.
28. Moreau, C., et al., *Dehydration of fructose to 5-hydroxymethylfurfural over H-mordenites.* Applied Catalysis a-General, 1996. **145**(1-2): p. 211-224.
29. Ilgen, F., et al., *Conversion of carbohydrates into 5-hydroxymethylfurfural in highly concentrated low melting mixtures.* Green Chemistry, 2009. **11**(12): p. 1948-1954.
30. Lansalot-Matras, C. and C. Moreau, *Dehydration of fructose into 5-hydroxymethylfurfural in the presence of ionic liquids.* Catalysis Communications, 2003. **4**(10): p. 517-520.
31. Qi, X.H., et al., *Catalytic dehydration of fructose into 5-hydroxymethylfurfural by ion-exchange resin in mixed-aqueous system by microwave heating.* Green Chemistry, 2008. **10**(7): p. 799-805.
32. Moreau, C., A. Finiels, and L. Vanoye, *Dehydration of fructose and sucrose into 5-hydroxymethylfurfural in the presence of 1-H-3-methyl imidazolium chloride acting both as solvent and catalyst.* Journal of Molecular Catalysis a-Chemical, 2006. **253**(1-2): p. 165-169.
33. Takagaki, A., et al., *A one-pot reaction for biorefinery: combination of solid acid and base catalysts for direct production of 5-hydroxymethylfurfural from saccharides.* Chemical Communications, 2009(41): p. 6276-6278.
34. Ohara, M., et al., *Syntheses of 5-hydroxymethylfurfural and levoglucosan by selective dehydration of glucose using solid acid and base catalysts.* Applied

Catalysis a-General, 2010. **383**(1-2): p. 149-155.

35. Huang, R.L., et al., *Integrating enzymatic and acid catalysis to convert glucose into 5-hydroxymethylfurfural.* Chemical Communications, 2010. **46**(7): p. 1115-1117.
36. Zhao, H.B., et al., *Metal chlorides in ionic liquid solvents convert sugars to 5-hydroxymethylfurfural.* Science, 2007. **316**(5831): p. 1597-1600.
37. Hu, S.Q., et al., *Efficient conversion of glucose into 5-hydroxymethylfurfural catalyzed by a common Lewis acid SnCl4 in an ionic liquid.* Green Chemistry, 2009. **11**(11): p. 1746-1749.
38. Sun, Y. and J.Y. Cheng, *Hydrolysis of lignocellulosic materials for ethanol production: a review.* Bioresource Technology, 2002. **83**(1): p. 1-11.
39. Graenacher, C., *US Patent, 1946176.* 1934.
40. El Seoud, O.A., et al., *Applications of ionic liquids in carbohydrate chemistry: A window of opportunities.* Biomacromolecules, 2007. **8**(9): p. 2629-2647.
41. Remsing, R.C., et al., *Mechanism of cellulose dissolution in the ionic liquid 1-n-butyl-3-methylimidazolium chloride: a C-13 and Cl-35/37 NMR relaxation study on model systems.* Chemical Communications, 2006(12): p. 1271-1273.
42. Yu, S., et al., *Single-step conversion of cellulose to 5-hydroxymethylfurfural (HMF), a versatile platform chemical.* Applied Catalysis a-General, 2009. **361**(1-2): p. 117-122.
43. Qi, X.H., et al., *Fast Transformation of Glucose and Di-/Polysaccharides into 5-Hydroxymethylfurfural by Microwave Heating in an Ionic Liquid/Catalyst System.* Chemsuschem, 2010. **3**(9): p. 1071-1077.
44. Binder, J.B. and R.T. Raines, *Simple Chemical Transformation of Lignocellulosic Biomass into Furans for Fuels and Chemicals.* Journal of the American Chemical Society, 2009. **131**(5): p. 1979-1985.
45. Takagaki, A., et al., *One-pot Formation of Furfural from Xylose via Isomerization and Successive Dehydration Reactions over Heterogeneous Acid and Base Catalysts.* Chemistry Letters, 2010. **39**(8): p. 838-840.
46. Gill, C.S., B.A. Price, and C.W. Jones, *Sulfonic acid-functionalized silica-coated magnetic nanoparticle catalysts.* Journal of Catalysis, 2007. **251**: p. 145-152.
47. Yurdakoc, M., et al., *Acidity of silica-alumina catalysts by amine titration using Hammett indicators and FT-IR study of pyridine adsorption.* Turkish Journal of Chemistry, 1999. **23**(3): p. 319-327.

48. Kao, H.M., et al., *One-pot synthesis of ordered and stable cubic mesoporous silica SBA-1 functionalized with amino functional groups.* Microporous and Mesoporous Materials, 2008. **113**(1-3): p. 212-223.
49. Rac, B., et al., *A comparative study of solid sulfonic acid catalysts based on various ordered mesoporous silica materials.* Journal of Molecular Catalysis a-Chemical, 2006. **244**(1-2): p. 46-57.
50. Hsu, W.H., et al., *Cellulosic Conversion in Ionic Liquids (ILs): Effects of H2O/Cellulose Molar Ratios, Temperatures, Times, and Different ILs on the Production of Monosaccharides and 5-Hydroxymethylfurfural (5-HMF).* Catalysis Today, 2011.